NeuroImage 146 (2017) 741–762

Contents lists available at ScienceDirect

NeuroImage

journal homepage: www.elsevier.com/locate/neuroimage

Age-dependent changes in task-based modular organization of the human brain

Kimberly J. Schlesinger[a,*], Benjamin O. Turner[b], Brian A. Lopez[b], Michael B. Miller[b], Jean M. Carlson[a]

[a] Department of Physics, University of California, Santa Barbara, CA, USA
[b] Department of Psychological & Brain Sciences, University of California, Santa Barbara, CA, USA

ARTICLE INFO

Keywords:
Aging
Dynamic networks
Modularity
fMRI

ABSTRACT

As humans age, cognition and behavior change significantly, along with associated brain function and organization. Aging has been shown to decrease variability in functional magnetic resonance imaging (fMRI) signals, and to affect the modular organization of human brain function. In this work, we use complex network analysis to investigate the dynamic community structure of large-scale brain function, asking how evolving communities interact with known brain systems, and how the dynamics of communities and brain systems are affected by age. We analyze dynamic networks derived from fMRI scans of 104 human subjects performing a word memory task, and determine the time-evolving modular structure of these networks by maximizing the multislice modularity, thereby identifying distinct communities, or sets of brain regions with strong intra-set functional coherence. To understand how community structure changes over time, we examine the number of communities as well as the flexibility, or the likelihood that brain regions will switch between communities. We find a significant positive correlation between age and both these measures: younger subjects tend to have less fragmented and more coherent communities, and their brain regions tend to change communities less often during the memory task. We characterize the relationship of community structure to known brain systems by the recruitment coefficient, or the probability of a brain region being grouped in the same community as other regions in the same system. We find that regions associated with cingulo-opercular, somatosensory, ventral attention, and subcortical circuits have a significantly higher recruitment coefficient in younger subjects. This indicates that the within-system functional coherence of these specific systems during the memory task declines with age. Such a correspondence does not exist for other systems (e.g. visual and default mode), whose recruitment coefficients remain relatively uniform across ages. These results confirm that the dynamics of functional community structure vary with age, and demonstrate methods for investigating how aging differentially impacts the functional organization of different brain systems.

1. Introduction

Humans experience notable changes in cognitive ability and behavior as they age, often in situations involving memory encoding, memory retrieval, and executive control functions (Balota et al., 2000; Grady and Craik, 2000; Cepeda et al., 2001; West et al., 2002; Treitz et al., 2007). Over the past few decades, advances in brain imaging have made it possible to observe and quantify neural changes associated with advanced age. One of the most widely-reported phenomena associated with aging is the loss of segregation between neural systems: many networks become less internally coherent, while at the same time they become more similar to other networks. This result has been reported using a number of methodological approaches, including whole-brain ICA (Onoda et al., 2012), whole-brain parcel-based functional connectivity methods (Betzel et al., 2014; Chan et al., 2014; Song et al., 2014; Ferreira et al., 2015; Geerligs et al., 2015) as well as similar analyses confined to a subset of systems (Grady et al., 2016; Ng et al., 2016), whole brain voxel-wise analyses (Tomasi and Volkow, 2012), and seed-based methods (Zhang et al., 2014) (for reviews, see Dennis and Thompson (2014), Contreras et al. (2015) and Sala-Llonch et al. (2015)). Moreover, these changes have been tracked longitudinally within participants (Ng et al., 2016), have been shown to affect various properties theoretically associated with the efficiency and efficacy of information processing in the brain (Sala-Llonch et al., 2014; Gomez-Ramirez et al., 2015), and have been associated with behavioral effects (Ng et al., 2016; Sala-Llonch et al., 2014).

* Corresponding author.
E-mail address: kschlesi@physics.ucsb.edu (K.J. Schlesinger).

http://dx.doi.org/10.1016/j.neuroimage.2016.09.001
Received 25 May 2016; Accepted 1 September 2016
Available online 03 September 2016

Although the dominant change associated with aging is one of decreased intra-network connectivity and increased inter-network connectivity, this pattern varies across networks. The loss of intra-network connectivity is found most consistently in the default mode network (DMN), even among those studies that consider brainwide connectivity (Onoda et al., 2012; Tomasi and Volkow, 2012; Wang et al., 2012; Song et al., 2014; Ferreira et al., 2015; Geerligs et al., 2015; Ng et al., 2016). Some studies also report similar decreases in networks associated with higher cognitive functions (Onoda et al., 2012; Wang et al., 2012; Chan et al., 2014; Geerligs et al., 2015; Ng et al., 2016). However, other networks consistently show no change, or even an increase in intra-network connectivity, especially those associated with sensory functions (Tomasi and Volkow, 2012; Song et al., 2014; Geerligs et al., 2015). Similarly, connectivity between the DMN and other networks tends to increase (or, equivalently, the uniqueness of the networks decreases) (Ferreira et al., 2015; Ng et al., 2016).

In parallel with this line of research on how the brain's functional architecture changes with age, a largely separate effort has sought to extend connectivity methods by accounting for the fact that the brain is not static (for a review, see Calhoun et al. (2014)). To the contrary, this work has demonstrated that patterns of connectivity are quite variable (Gonzalez-Castillo et al., 2014), which can be characterized as constituting a series of transitions between fairly well-defined brain states (Hansen et al., 2015). It has been proposed that the greatest variability occurs in regions that serve to connect fairly well-segregated systems (Zalesky et al., 2014), and that a small set of networks may modulate the organization across a large number of others (Di and Biswal, 2015). The time-resolved approach adds yet another dimension for investigating age-related effects; for example, Qin et al. (2015) report increased variability in connectivity across networks including DMN and cerebellum, and decreased variability between those two and within the cingulo-opercular network, as a function of age.

Having established these aging-related changes in functional connectivity—along with some general principles of dynamic connectivity—in the resting state, an obvious next question is how the results differ during task performance. “Task-free” paradigms dominate studies of functional connectivity. Incorporating a task could affect connectivity, including its relationship with age and its dynamics, in a number of ways. For instance, compensatory strategies employed by older—but not younger—adults could drive the connectivity profiles of the two groups even further apart; alternatively, the presence of an extrinsic input could impose structure on the systems that have become homogenized in older adults. Indeed, Dubois (2016) demonstrated widespread changes in the relationship between age and connectivity across resting and task scans, with the largest effects being a weakening in the age–connectivity relationship during tasks compared with rest. Likewise, connectivity between and within networks could change as participants learn, change strategies, or even simply become fatigued.

For the present study, we used a memory task that incorporated a strong element of cognitive control. In particular, after studying a list of items, participants were presented with the studied items, along with novel (unstudied) items, and instructed to indicate whether each item was studied or not. Items occurred in one of two contexts: a “liberal” context indicating that each item in that context was likely to have been studied (70% of items were studied items) or a “conservative” context indicating that each item was unlikely to have been studied (30% of items studied). In the face of imperfect memory evidence, participants must exert cognitive control—adjusting the criterion they use to endorse an item as studied—in order to perform well on this task. Given that the domains of memory and cognitive control are fundamental in human cognition, and are associated with changes over the lifespan (Jacoby et al., 2005), this task is an appealing choice for studying how the brain's architecture changes with age when *not* at rest. Previous results with this task revealed wide individual differences in adaptability (Aminoff et al., 2012), and implicated a network of regions including lateral prefrontal and lateral posterior parietal cortex in performing this task (Aminoff et al., 2015).

Although the brain regions associated with the performance of this task are well documented, these results are derived from the standard mass-univariate GLM analysis of BOLD data, and therefore give little basis for predictions in terms of network-level dynamics. In fact, by definition, these existing results assume stationarity and consider each voxel as independent. Even results derived from methods that explicitly model the spatiotemporal nature of brain activity (e.g., ICA) would require a theoretical framework in order to define regions of interest in the context of how network dynamics relate to other factors, such as age. Thus, there remains a gap in understanding of the neural processes related to performance of this task on the level of dynamic interactions between large-scale brain regions and networks. Our current understanding of these processes, based on existing theories and results, is specified on a very different level from the target of our current investigation. Our goal in this work is to apply a data-driven analysis method to investigate the dynamics of these regions and networks, which allows us to uncover age-related changes at scales at which it is difficult to make specific hypotheses based upon existing literature.

We apply a dynamic community detection method to quantify several higher-order aspects of task-based functional connectivity and their dependence on age. This method and other network science approaches have proved successful in distilling the information in fMRI data into intuitive, descriptive, and predictive network characteristics (Bassett et al., 2012; Davison et al., 2015; Siebenhühner et al., 2013; Bullmore and Sporns, 2012; Bassett et al., 2009, 2011, 2015). While previous results suggest that static community structure will meaningfully differ on a group level between older and younger adults at rest (Meunier et al., 2008), we ask whether the dynamic changes in these communities are affected by age during task-based cognition, and how such effects vary across individual participants. We quantify the size and number of functional brain communities, the degree to which brain regions flexibly switch between communities, and the association of the community structure with known intrinsic functional connectivity networks or systems, in order to determine whether these systems are differentially involved in age-related changes.

2. Materials and methods

2.1. Participants

126 participants were recruited from the UCSB and Santa Barbara communities and scanned at the UCSB Brain Imaging Center. 22 subjects were not included in this analysis due to technical issues, metal screening issues, claustrophobia, and attrition. The 104 participants assessed here came from three separate age groups: 35 adolescents (age 18, 18 female), 34 young adults (ages 25–33, mean age 28.5, 16 female), and 35 older adults (ages 60–75, mean age 67.2, 18 female). All subjects had a history of normal memory ability for their age, and a Mini-Mental State Examination score of 27 or above (Turner et al., 2015; Folstein et al., 1975). All subjects gave informed written consent prior to experimental procedures and were paid for their participation. All procedures were approved by the University of California, Santa Barbara Human Subjects Committee.

2.2. Stimuli and procedure

Subjects performed a recognition memory task designed to test memory for words and to measure how participants strategically use probabilistic information as a supplemental guide to memory (Aminoff et al., 2012). During a study session (which occurred inside the scanner, immediately before beginning scanning), subjects were asked to memorize a list of 153 common English words. Subjects were then scanned during three consecutive test sessions, each consisting of 102 trials (each spanning a single TR) in which subjects were shown a word

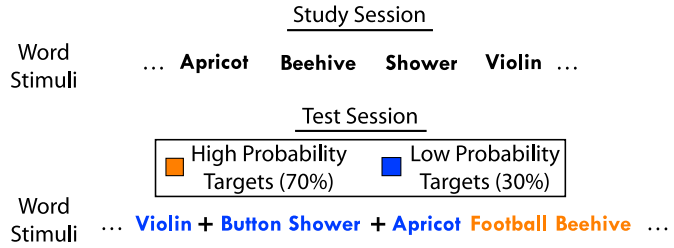

Fig. 1. Memory task structure. A schematic depiction of the word memory task design. During a study session, subjects study a list of common words. They are then scanned during the study session, in which they are shown a new set of words and asked to decide whether each word has been seen before in the study session. Words in the test session are colored to provide probabilistic information about their likelihood of having been seen in the study session.

and asked to indicate whether they had seen that word in the study session, interspersed with 214 blank jitter TRs.

The test session word stimulus in each trial was presented with probabilistic information about the correct response; words of one color (blue or orange, counterbalanced across subjects) had a 70% probability of having been presented in the study session, and words of the other color a 30% probability. These probability contexts were presented in a blocked fashion, such that the probability context changed every 5–7 trials. Half of the trials in each functional run (51 words) were studied, while the other half were unstudied. A schematic of the task design is shown in Fig. 1 (Aminoff et al., 2012). For more information on the details of the procedure, see Ref. Turner et al. (2015).

2.3. Imaging acquisition and preprocessing

Subjects were scanned with a 3T Siemens TIM Trio MRI system with a standard 12-channel head coil. Functional data were collected with a T2*-weighted echo-planar sequence (30 interleaved slices, 3 mm thickness, 3 × 3 mm in-plane resolution; TR=1.6 s; TE=30 ms; FA=90) with generalized autocalibrating partially parallel acquisitions (GRAPPA). A high-resolution anatomical image was collected at the beginning of the scanning session for each participant using an MPRAGE sequence (TR=2.3 s; TE =2.98 ms; FA=9°; 160 slices; 1.1 mm thickness). Additionally, diffusion-tensor imaging and resting state fMRI scans were acquired but are not considered further here.

The data were preprocessed using FEAT v6.0, part of FSL Jenkinson et al., 2012. Preprocessing included motion correction with MCFLIRT, non-brain removal with BET, spatial smoothing (FWHM=5 mm), high-pass temporal filtering (σ=50 s), and grand mean intensity normalization. The mean relative motion across all TRs, averaged across functional runs, was also recorded for each subject. It has previously been established that motion varies reliably with age (Turner et al., 2015), so all subsequent analyses are conducted with mean motion partialed out.

The data were then processed further using a nuisance regression with the following regressors: the six relative motion correction terms returned by MCFLIRT, their temporal derivatives, and the mean signal timecourse from cerebrospinal fluid (generated by segmenting the high resolution T1 image, thresholding the CSF probability image at 0.9, and taking an average over all in-mask voxels). The model also included regressors for each probability context block, which were modeled as a boxcar of duration equal to the context, convolved with an HRF (gamma model, phase=0 s, standard deviation=3 s, mean lag=6 s), plus temporal derivatives. To generate the final denoised data, we took the residuals of this model with respect only to the motion and CSF regressors. Finally, the denoised data were registered to MNI space using FLIRT. First, the high resolution T1 image was registered to the MNI template (12 *df* affine transformation), then the functional data were registered with the high resolution image (6 *df* affine transformation, trilinear interpolation), and the transformations were combined.

2.4. Creating dynamic brain networks

In order to investigate the large-scale network structure of brain activity, a dynamic network was constructed separately from each subject's measured functional activity. Each network is defined as containing n nodes, treated as constant over time. Here these nodes consist of the n=194 regions of a "hybrid" anatomical atlas, an adaptation of the multi-resolution Lausanne2008 atlas minimizing cross-brain and inter-subject variability in region size (Davison et al., 2015; Hagmann et al., 2008). This atlas was registered to MNI space. Node-specific time series from each functional run were generated for each node by averaging the time series of all voxels within the node (Davison et al., 2015).

Each network has $e = n(n-1)/2$ edges, each with a real-valued, non-negative connection weight that may change dynamically over time, taking on a new value in each of T sequential time windows spanning the experiment. The weight of an edge between nodes i and j in a given time window l, denoted A_{ijl}, is defined as the mean low-frequency (0.06–0.125 Hz) wavelet coherence between the BOLD time series of i and j within time window t Grinsted et al., 2004. Edge weights are always valued in [0, 1]. In this study, we investigate two separate time window sizes. We focus primarily on windows containing 52 time samples (18 windows in total), with each window representing approximately 80 s or 1.3 min. We also analyze for comparison the results from more temporally coarse-grained windows containing 316 time samples (3 windows in total), with each window representing approximately 500 s or 8.4 minutes, the length of a single functional run of the experiment. Note that these window sizes are both significantly longer than individual trials (each of which contains one word stimulus and one decision, and lasts for approximately 2 s), as well as blocks of trials belonging to each of the two probability conditions (which contain about six trials each and are approximately 12 s long); we make this choice in order to ensure that each window contains sufficient time sampling statistics to provide a reliable estimate of the coherence or edge weight within that window (Davison et al., 2015; Bassett et al., 2015, 2011).

2.5. Detecting dynamic community structure

To study the time-evolving modular structure of these networks, we identify distinct communities, or sets of brain regions with strong intra-set functional coherence, and quantify how these communities change over time. For each subject's dynamic network, a community partition is determined by maximizing the multislice modularity Q, a function indicating the quality of the modular structure of a given partition of the network, in comparison to that expected of a randomized "null" network (Mucha et al., 2010). The multislice modularity of a network partition is given by

$$Q = \frac{1}{2\mu} \sum_{ijlr} \{(A_{ijl} - \gamma_l P_{ijl})\delta_{lr} + \omega_{jlr}\delta_{ij}\}\delta(g_{il}, g_{jr}). \quad (1)$$

Here, the Kronecker delta $\delta(g_{il}, g_{jr})$ is equal to 1 when the community assignment of node i in window l (g_{il}) is the same as the community assignment of node j in window r (g_{jr}); otherwise, it takes a value of 0. A_{ijl} is the edge weight between nodes i and j in time window l, as defined above; P_{ijl} is the corresponding edge weight in the null network, with a spatial resolution factor γ_l determining the relative weight of the null model within in each time window (see Section 2.1 of Appendix for details). Thus, the first term in brackets provides a positive contribution to Q, for each pair of nodes assigned the same community in the same time window, proportional to the difference between the actual edge weight between the pair and that in the weighted null model. The second term in the brackets includes a time resolution factor ω_{jlr} for each node j and each pair of time windows l and r (see Section 2.1 of Appendix for details). This term provides a

positive contribution of ω to Q, for each node j and each pair of time windows l and r, when j is assigned to the same community in both time windows. μ is a normalizing factor given by $\mu = \frac{1}{2}\sum_{jl} \kappa_{jl}$, where $\kappa_{jl} = c_{jl} + k_{jl}$, $c_{jl} = \sum_r \omega_{jlr} = \omega T$, and $k_{jl} = \sum_i A_{ijl}$, or the weighted degree of node j in time window l (Mucha et al., 2010).

This multislice modularity is larger for community partitions that group together nodes with comparatively strong pairwise edge weights (as compared to the null network) within each window, and that group more nodes in the same community as themselves across multiple time windows. In this study we use the Newman-Girvan null model, in which $P_{ijl} = \frac{k_{il}k_{jl}}{2m_l}$ and $2m_l = \sum_{ij} A_{ijl}$; this commonly used choice of null model treats the measured edge weights as randomly distributed within each window while preserving the node degree distribution. We maximize Q over partitions with a Louvain-like locally greedy algorithm (Mucha et al., 2010; Blondel et al., 2008). Due to the stochasticity of the algorithm and the expected high degeneracy of solutions near the maximum value of Q, we use a community consensus procedure to distill a statistically representative partition from an ensemble of 100 solutions (Bassett et al., 2013).

2.6. Brain network community structure diagnostics

2.6.1. Basic community structure

We use several measures to quantitatively describe the dynamic community structure of each network, and to compare subjects' networks to each other.

The first set of metrics involves the number of distinct communities in a subject's brain network. The number of *dynamic communities* is evaluated over the entire dynamic network, and counts each community that appears in at least one time window. Communities which stretch over several time windows, but are associated together under the same community label, are counted as only one dynamic community. (Note that the community detection algorithm automatically identifies communities in each window with those that have similar membership in other time windows, and assigns them the same label; this self-identification is enforced to an extent controlled by the strength of the inter-window coupling parameter ω). In contrast, the number of *static communities* is evaluated within each time window separately, counting each distinct, dynamically detected community appearing within that time window once, regardless of whether that community spans multiple time windows. Because communities may appear or disappear between windows, the dynamic community number and the static community numbers need not be equivalent.

The *flexibility* f of a node i within a network is defined as the number of times that node switches communities between all distinct pairs of time windows, normalized by the total possible number of switches:

$$f(i) = \frac{1}{T(T-1)} \sum_{t \neq t'} [1 - \delta(g_{it}, g_{it'})]. \tag{2}$$

Here, t and t' both run from 1 to T, the total number of time windows; $\delta(g_{it}, g_{it'})$ equals 1 if node i is assigned to the same community in time window t and time window t', and 0 otherwise. A node with high flexibility changes communities in every or nearly every time window and has a flexibility at or near 1, while a node with low flexibility may remain in the same community in all windows and have a flexibility of 0. We further define the *community flexibility* as the mean flexibility of all nodes in a particular community.

This method of computing "categorical" flexibility compares nodes between every possible pair of time windows, in contrast to "time-ordered" flexibility, which compares only time-adjacent windows. While many applications of categorical flexibility are used to compare communities across categories or tasks, we use categorical flexibility here to emphasize the consistency of nodes across long time windows which are statistically identical in terms of task design (for 500-s windows) or nearly so (for 80-s windows), without an assumed change in brain dynamics over time in the experiment. All results reported in this work are essentially unchanged when using time-ordered flexibility (see Section 2.2 of the Appendix).

2.6.2. Comparing communities to functional systems

To understand how the community structure of this data corresponds to known functional brain systems, we compare the community partitions to a basic *functional system partition* of the nodes. Based on the primary functional roles of different anatomical brain areas as reported in the literature, and as detailed in Gu et al. (2014) and Bassett et al. (2014), each node is assigned to one of ten functional systems: auditory, cingulo-opercular, default mode, dorsal attention, fronto-parietal, somatosensory, subcortical, ventral attention, visual, and other. These systems have been distilled using a network-based clustering approach (Power et al., 2011) and used to describe and quantify system-specific functional interactions in the brain (Power et al., 2013; Cole et al., 2013, 2014). The relationship of these functional systems to the community structure is described by the following quantitative metrics.

The *recruitment coefficient* of a given node is a measure of the consistency with which that node is grouped in the same community as other nodes within its own functional brain system. It is given by

$$R(i) = \frac{1}{n(s_i) - 1} \sum_{j \neq i} P(i,j)\delta(s_i, s_j), \tag{3}$$

where $\delta(s_i, s_j)$ equals 1 if the system of node i (denoted s_i) and the system of node j (denoted s_j) are the same, and 0 otherwise; $n(s_i) = \sum_j \delta(s_i, s_j)$, or the number of nodes in system s_i; and $P(i,j)$ is the frequency with which node i and node j are grouped in the same community (Gu et al., 2014; Bassett et al., 2014). Specifically, $P(i,j)$ is computed as the observed proportion of instances (i.e. time windows or modularity-optimizing partitions) in which i and j are placed in the same community.

We further define the *self-recruitment* Ψ of a given system S as the average recruitment coefficient of all nodes in the system, given by

$$\Psi(S) = \frac{1}{n(S)(n(S)-1)} \sum_{ij, i \neq j} P(i,j)\delta(s_i, S)\delta(s_j, S). \tag{4}$$

This measures the extent to which nodes in system S are cohesively grouped together in the same community (Gu et al., 2014; Bassett et al., 2014).

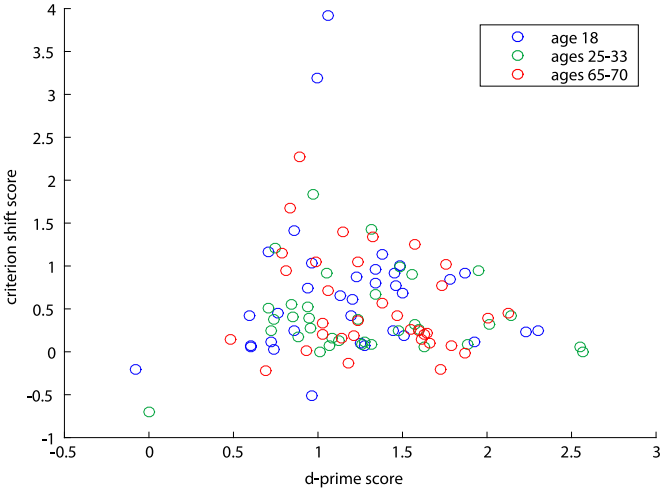

Fig. 2. Memory task performance measures. Distributions of d-prime and criterion shift scores for N=104 subjects. These measures characterize overall accuracy and the extent to which subjects switched strategies between probability contexts, respectively. Subjects are colored by age: blue indicates adolescents (age 18), green young adults (ages 25–33), and red older adults (ages 60–75). There is no apparent correlation between these measures (Pearson's $r = -0.060$, $p > 0.1$).

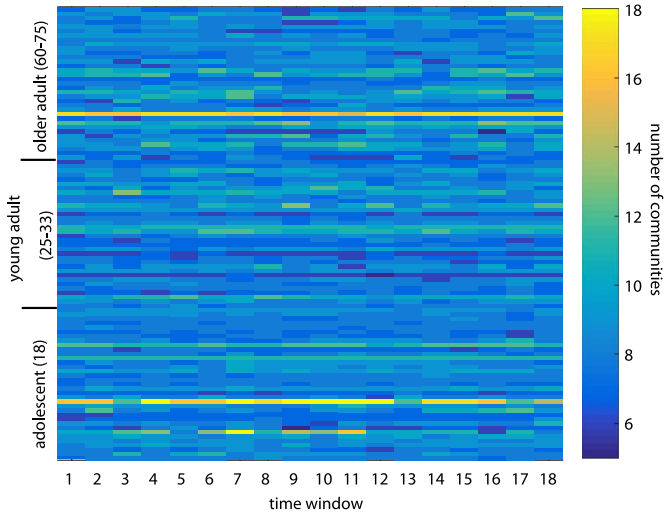

Fig. 3. Number of communities. Color indicates the number of communities detected within each 80-s time window in each subject. Subjects (on the vertical axis) are ordered by age. Notable individual differences exist between subjects, but community number changes comparatively little over the course of the experiment within individual subjects.

2.6.3. Correcting for mean relative motion

As mentioned above, subject age is correlated with mean relative motion in these data (Spearman's $\rho = 0.48$, $p = 1.80 \times 10^{-6}$), as found previously in ref. Turner et al. (2015). Thus, all subject-wise correlations presented here are performed with mean relative subject motion partialed out – i.e., each correlation variable was first regressed separately on mean relative motion, and we assessed the correlation between the residuals of these regressions, to ascertain the extent of their relationship that could not be explained by motion. Since subject age is significantly correlated with mean relative motion, it is possible that motion also affects the correspondence measures of community dynamics and age, and potentially other performance and demographic measures as well, due to the broad and non-uniform distribution of ages in our sample. Section 2.5 of the Appendix provides further details on the results of this correction.

3. Results

In this section, we present the characteristics of dynamic community structure within individuals, and evaluate their correspondence with age and recognition memory performance.

For assessing correlations with age throughout this section, we use the Spearman rank correlation, due to the non-continuity and non-uniformity of the ages in our subject sample. However, we use the Pearson correlation for assessing correlations with all performance measures, which are continuously and approximately normally distributed. We partial out mean relative motion from all subject-wise correlations, as discussed in Methods, and apply a Bonferroni correction for multiple comparisons on the set of overall and system-specific correlations for each pair of measures (e.g. age and flexibility, age and community number, criterion shift score and flexibility, etc.).

3.1. Word memory performance

We examine two behavioral measures of performance on the word memory task: d-prime, an indicator of overall accuracy on all memory trials; and criterion shift score, which describes the extent to which subjects change their response strategies in the face of probabilistic information about the correct responses (Aminoff et al., 2012). A more positive criterion shift score indicates that the subject made a comparatively large shift from a liberal to a conservative strategy when responding to high- and low-probability targets, respectively. A more negative criterion shift score indicates the opposite strategy shift (from conservative responses on high-probability targets to liberal responses on low-probability targets). Very few subjects displayed this objectively worse strategy. A criterion shift score of 0 indicates no strategy difference between high- and low-probability targets. We find that among all subjects in this study, the d-prime and criterion shift scores are approximately normally distributed, and they are not significantly correlated with each other (Fig. 2). In addition, neither measure shows any significant correlation with subject age Turner et al., 2015. Upon exclusion of two apparent outliers in Fig. 2, these results and the significance of other task performance correlations reported in the paper are not affected (see Section 2.4 of Appendix for details).

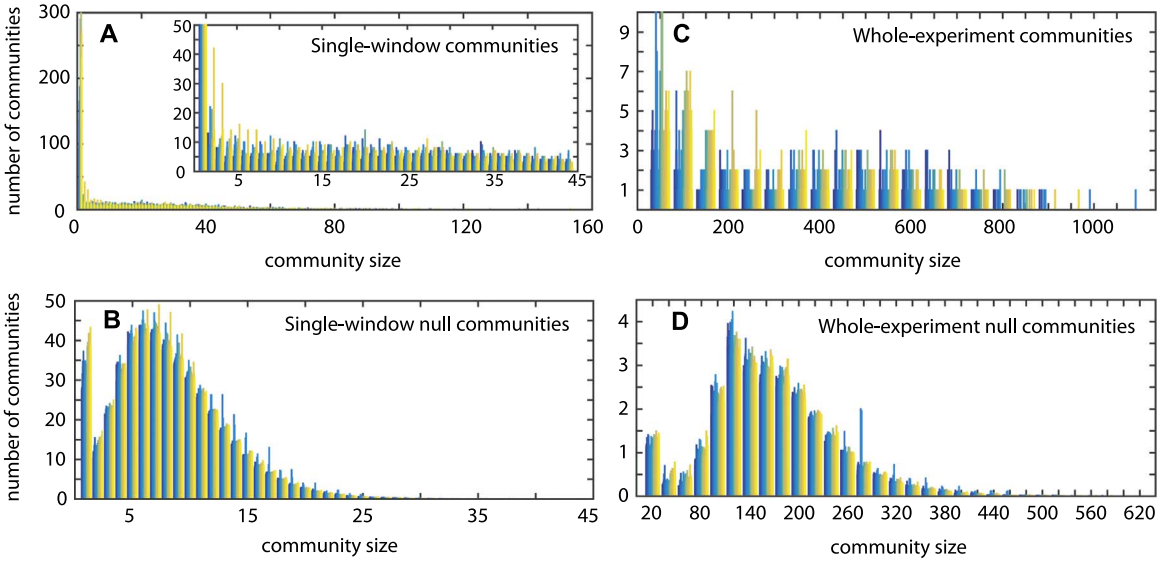

Fig. 4. Community size distributions. A and B show histograms of community sizes within individual time windows, for the observed data and averaged over 100 null networks, respectively. Values are plotted individually for each subject, each represented by one color. The inset shows the data in A restricted to the same axes as B for comparison. C and D show histograms of the sizes of dynamic communities across the whole experiment, also comparing observed data (C) to an average over 100 null networks (D). Community sizes tend to be larger at maximum and to be distributed much more evenly in functional brain networks than in randomized null models.

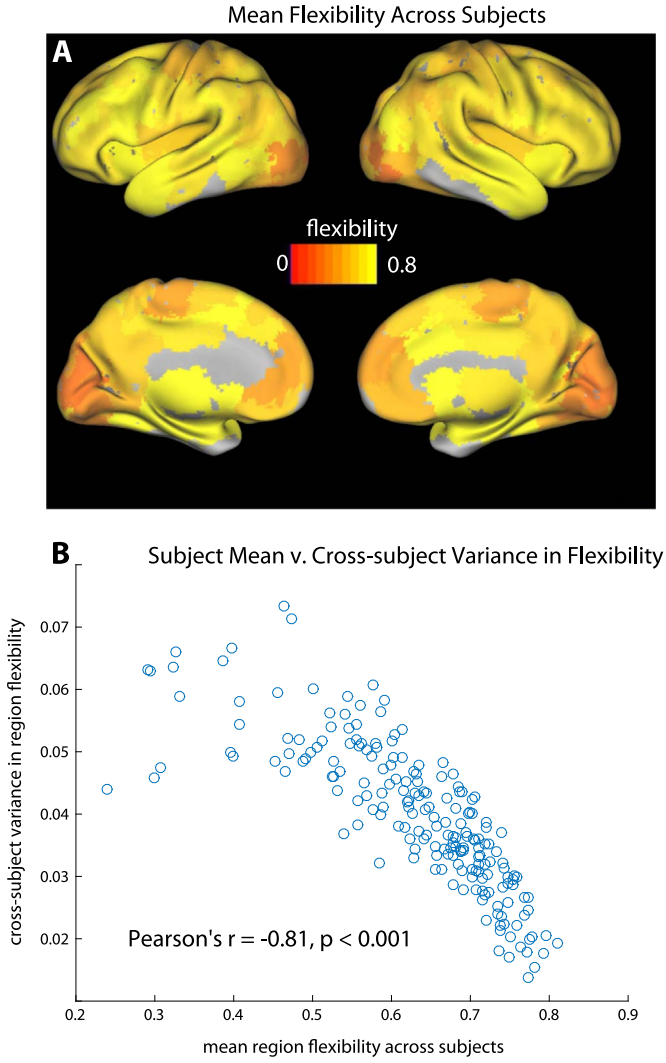

Fig. 5. Brain region flexibility. A: Flexibility of the 194 brain regions used as network nodes (mean over N=104 subjects). Visual cortex and somatosensory regions in particular have exceptionally low mean flexibility. B: Scatter plot of mean region flexibility against variance in region flexibility across subjects. Brain regions that are more flexible on average have a strong tendency to also display lower cross-subject variability in flexibility.

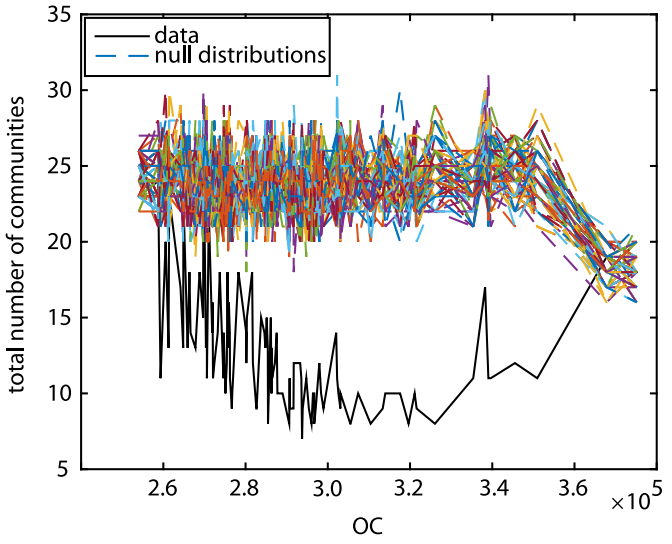

Fig. 6. Total community number and null distributions. Total number of communities identified in the brain network of each subject (solid black line) compared with total number of communities identified in each of 100 overall-connectivity-preserving null model networks for the same subjects (dashed colored lines). Subjects are sorted by overall connectivity (OC). The numbers of communities identified in the data are very different for most subjects from those found in null distributions with identical OC, suggesting that the communities detected are driven largely by characteristics of the underlying connectivity structure that cannot be explained by OC. The relationship between OC and number of communities appears to be nonlinear, with large and small OC tending to lead to numbers of communities that are more strongly driven by the OC value (i.e., more similar to the null model that preserves OC alone).

3.2. Functional communities in the brain

We focus primarily on the dynamic community structure of individual functional brain networks composed of time windows containing 52 time samples each. The experiment contains a total of 18 such time windows; each window represents functional connectivity within an approximately 80-s period. Community dynamics on time scales between 60 and 200 s provide relatively fine time resolution while retaining sufficient time sampling statistics within each window, and have been shown to contain relevant information about brain function in previous studies (Davison et al., 2015; Bassett et al., 2015, 2011). The 80-s windows used here are significantly longer than individual trials (approximately 2 s each) or blocks of trials sharing the same probability condition (approximately 12 s each). While they cannot resolve functional dynamics related to a specific word or probability condition, these windows are expected to capture the cognitive control and memory processes that are active over the course of several strategy blocks in the task.

For comparison, we also investigate the community dynamics of networks composed of much longer time windows, each containing 316 time samples and corresponding to one functional run of the experiment. The time windows in these networks capture dynamics over a longer time scale, with each window representing approximately 500 s or 8.4 min of brain activity, and a total of only three windows across the experiment. The results in these 500-s networks are in general qualitatively similar to results from 80-s networks, although the correspondences between demographics or performance measures and community dynamics are often much weaker. This suggests that shorter (80-s) time windows resolve the relevant dynamics better than longer windows. The shorter time windows are also somewhat closer in length to the timescales of cognitive function demanded by the task setup (although still not identical or aligned with blocks of probability context or other specific task features). Therefore, in this Results section we focus on networks with 80-s time windows, except where explicitly noted. Results from 500-s time windows are presented in Section 1 of the Appendix.

3.2.1. Number and size of communities

Fig. 3 shows the number of static communities identified in each 80-s time window of the functional brain networks during the memory task in each subject. (Here “static communities” refers to the number of distinct, dynamically detected communities present in a single given time window, while “dynamic communities” counts the total number of communities identified by dynamic community detection in all time windows.) For almost all subjects, the number of static communities remains fairly stable across time windows, and the number of dynamic communities is only slightly larger than the number in any one window. This indicates that few communities appear or disappear, and that community number is a measure with more meaningful individual, inter-subject differences than time-dependent intra-subject differences.

Each subject has between 7 and 24 total dynamic communities (mean=12.7). The correlations with community number in the remainder of this work use each subject's dynamics community number as the primary measure, since it corresponds closely with static community number throughout the experiment.

Note that in Fig. 3, two subjects in particular appear to have much

Table 1
Correlations between subject age and community measures. Spearman rank correlation ρ values and associated p-values for correlations between age and each of three community metrics: community number, flexibility, and age. Mean relative motion has been partialed out of all correlations. Italics indicate correlations that are not significant ($p > 0.05$) after family-wise error rate correction for multiple comparisons within each column; all non-italicized values represent significant correlations ($p < 0.05$).

	Community No.		**Flexibility**		**Recruitment**	
	ρ	p-value	ρ	p-value	ρ	p-value
Whole brain	0.28852	0.0031207	0.52984	8.66E-09	−0.32053	9.64E-04
Auditory	0.38723	5.33E-05	0.49118	1.38E-07	−0.21268	3.10E-02
Cingulo-opercular	0.35580	2.26E-04	0.55497	1.18E-09	−0.31670	1.12E-03
Default Mode	0.40296	2.44E-05	0.44264	2.84E-06	−0.22947	1.97E-02
Dorsal Attention	0.30945	1.47E-03	0.36514	1.49E-04	−0.06906	4.88E-01
Fronto-parietal	0.31721	1.10E-03	0.53856	4.41E-09	−0.22348	2.33E-02
Other	0.35313	2.53E-04	0.44943	1.92E-06	−0.14008	1.58E-01
Somatosensory	0.39382	3.86E-05	0.46037	9.94E-07	−0.31483	1.20E-03
Subcortical	0.38995	4.67E-05	0.46622	6.93E-07	−0.29679	2.33E-03
Ventral Attention	0.39083	4.47E-05	0.32840	7.07E-04	−0.33822	4.75E-04
Visual	0.37777	8.36E-05	0.27263	5.34E-05	−0.15554	1.17E-01

higher static community numbers than the others, and are potential outliers in this regard. Nearly all results pertaining to the correspondence between age, performance, and community structure reported herein remain unchanged when these subjects are removed from the analysis. One discrepancy is noted below and further details are provided in Section 2.4 of the Appendix.

Figs. 4A and C show the distribution of community sizes for each individual, both within individual time windows and across the entire experiment. Community sizes are relatively uniformly distributed, save for an excess of communities of very small size. Results with single-node communities, or "singletons," excluded from the analysis do not differ substantially from those reported here; see Section 2.3 of the Appendix for further details on singletons.

3.2.2. Flexibility

Fig. 5A shows the flexibility of each of the n=194 brain regions, averaged over N=104 subjects, for networks with 80-s time windows. Regions in the occipital lobe, most of which are in visual cortex, tend to show relatively low flexibilities, as do some motor-associated regions in the dorsal anterior frontal and posterior parietal lobes. Most other brain regions have a somewhat higher flexibility. Consistent with previous work (Bassett et al., 2011), we find notably greater variation in flexibility across subjects than across brain regions.

We find that the regions with lower mean flexibility across subjects tend to have a higher cross-subject variance, as shown in Fig. 5B; in other words, highly flexible nodes are very consistently flexible across subjects, while nodes with lower mean flexibility (such as those in visual and motor cortex) show greater individual differences in dynamics.

This effect differs strikingly from the flexibility patterns seen on longer timescales, in networks composed of 500-s time windows. The identities of the brain regions with the lowest mean flexibility and the variance of those regions are very similar with both 80-s and 500-s time windows. However, with 500-s time windows, the cross-subject variance of the high-flexibility (non-visual, non-motor) regions is much higher than that of the same regions in networks with 80-s time windows, and consistently higher than the variance of low-flexibility regions as well (see Appendix for further discussion).

3.2.3. Dependence of community structure on overall brain connectivity

In our sample, we find considerable variation in the density of subjects' functional networks, computed as the sum of all functional connectivity weights between brain region pairs. That is, some subjects have higher overall brain connectivity or coherence than others. In addition, we find that this overall connectivity (OC) is significantly correlated with subject age (Spearman's $\rho = -0.50$, $p < 0.001$).

To ensure that the community structures we identify are not primarily driven by OC alone, but instead capture underlying dynamics in functional connectivity, we construct a null model in which we destroy the underlying connectivity structure in each subject by redistributing network edge weights among region pairs uniformly at random, preserving only the symmetry of the edge matrix, the lack of self-edges, and the total sum of edge weights (i.e., overall connectivity) in each time window of each subject's network. Note that this null model also destroys the inherently constrained structure of the coherence matrix, such that the randomly permuted matrices are not necessarily examples of coherence matrices, as the original networks are. This null model thus cannot speak to the inherent effect of coherence structure on community structure, but can only elucidate density effects.

We create 100 randomly permuted null networks for each subject, and analyze the communities identified therein. As shown in Fig. 6, the null distributions of total community number are relatively uniform across subjects, save the two subjects with the highest OC, who display consistently lower community number across null networks. A non-linear relationship between OC and the number of communities identified is evident here–in contrast to this behavior at high OC, the number of communities increases with increased OC at the low-OC end of the distribution.

For most subjects, the number of communities identified in Fig. 6 is smaller and differs fundamentally from the number identified in randomized networks. There is no significant correlation between a subject's number of communities and the mean number of communities identified in the corresponding networks. However, if the two outlier subjects with high OC are excluded, the number of communities in null models preserving only by OC does significantly correspond to the mean number of communities in subjects' brain networks (Pearson's r=0.32, $p < 0.001$).

The distributions of community sizes for each subject, shown in Figs. 4A and C, are in general relatively uniform, save for elevated numbers of communities of small sizes. Null networks (Figs. 4B and D) show very different community size distributions, which include a clear peak at intermediate sizes and much smaller maximum community sizes. These stark differences show that while some aspects of the community structure are related to OC, others are driven by characteristics of the underlying connectivity structure that cannot be explained by OC alone.

3.3. Relationship of functional community structure to age and performance

Analysis of community number and flexibility distributions reveals that both measures vary across subjects notably more than across time

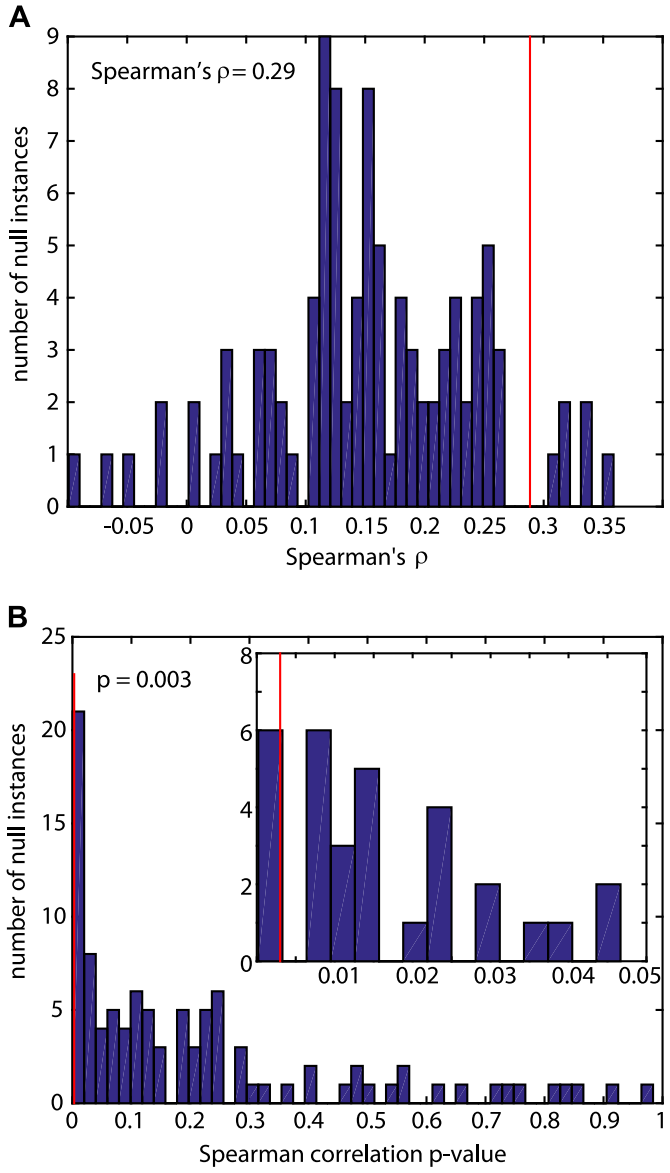

Fig. 7. Relationship between age and number of communities in functional brain data and corresponding null models. A: The solid red line shows the Spearman correlation value between subject age and number of communities; the bars show a histogram of the same correlation values, each computed from one set of 100 OC-preserving null networks. B: The solid red line shows the *p*-value of the Spearman correlation observed in the data; the bars show the null distribution of *p*-values corresponding to the null Spearman correlation values in A. For six out of 100 randomized community structures, the correlation between age and number of random communities is stronger than the observed correlation between age and number of functional brain communities. However, for most randomized community structures, no significant correlation is found between age and number of random communities is found.

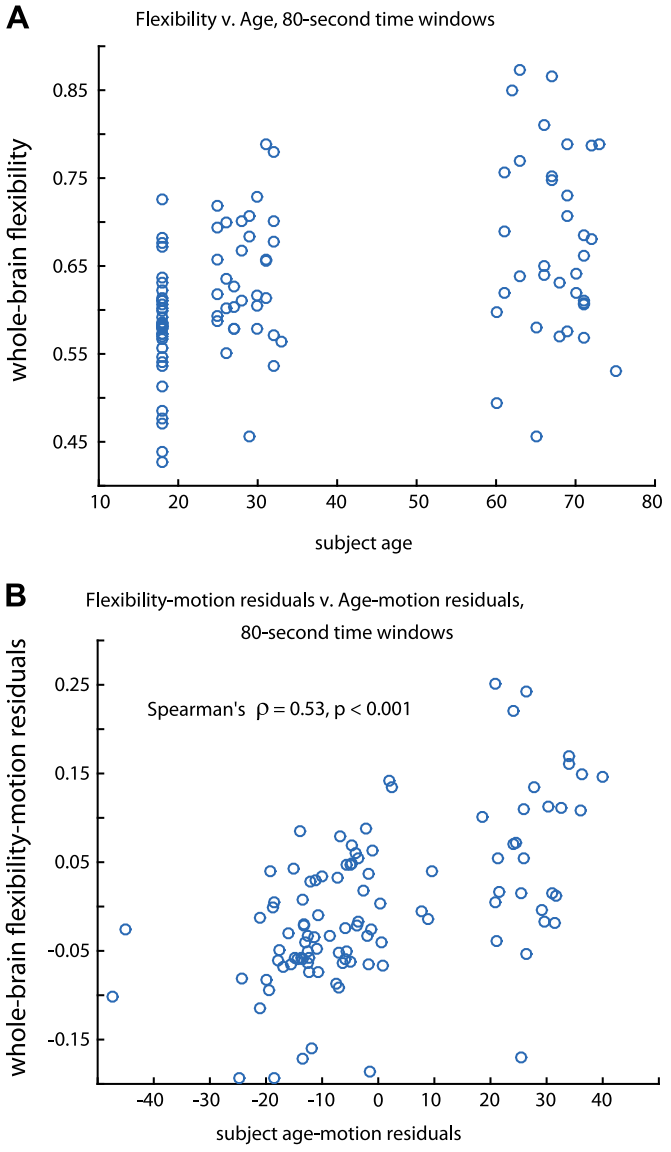

Fig. 8. Whole-brain flexibility and age. A: Scatter plot of the correspondence between subject age and whole-brain flexibility in networks with 80-s time windows. B: Scatter plot showing the significant positive correlation between age and whole-brain flexibility with mean relative motion partialed out (plot shows residuals of separately regressing each measure on mean relative motion).

windows or brain regions within individual subjects. We investigate these individual differences in community number and flexibility, and whether they are related to age or performance, by examining the *total community number* in each subject's entire time-dependent functional network, as well as the *whole-brain flexibility* of each subject, or the mean flexibility over all that subject's nodes. Here we summarize the results of these comparisons, which are also presented in Table 1.

We find that total community number is significantly positively correlated with subject age (Spearman's $\rho = 0.29$, $p < 0.05$). This indicates that cohesive functional communities in the brains of older subjects tend to be more fragmented than those in younger subjects. A significant correlation between community number and age (Spearman's $\rho = 0.31$, $p < 0.05$) is also seen on average in null networks that preserve OC but randomize other topological/spatial network structure. Six out of 100 instances of randomized networks have a stronger Spearman correlation between age and total number of randomized communities than the correlation between age and number of communities reported above (Fig. 7).

We find that whole-brain flexibility is also significantly positively correlated with age, as shown in Fig. 8 (Spearman's $\rho = 0.53$, $p < 0.001$). This indicates that younger subjects have brain regions that switch between communities significantly less frequently, and thus more stable community partitions over the course of the experiment.

We find no significant correlations between task performance metrics – either d-prime or criterion shift score – and any of the three metrics of community dynamics, including flexibility, number of communities, and recruitment. This holds true for global brain metrics and for those localized to specific functional systems. In addition, we conduct a multivariate regression analysis to test whether task performance is predictive of brain metrics in individual brain regions. This analysis uses the flexibility scores of the 194 nodes in all subjects as outcomes, and the two performance metrics – d-prime and criterion

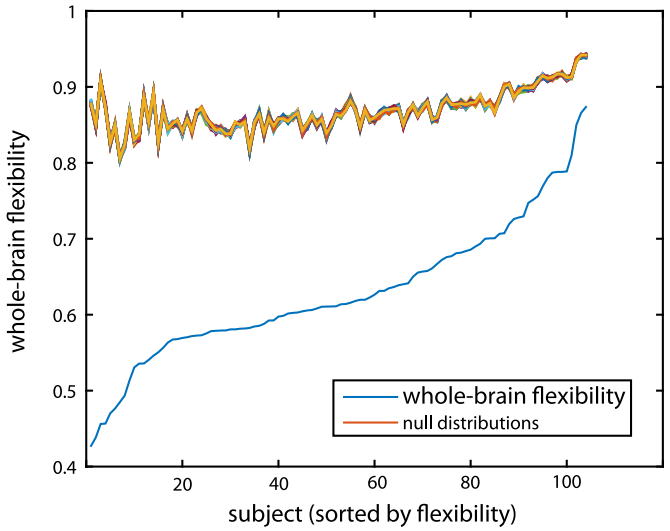

Fig. 9. Whole-brain flexibility and null distributions. The solid black line shows the whole-brain flexibility of each subject (sorted); the colored lines show the distribution of whole-brain flexibilities computed from 100 instances of the corresponding community-number-preserving null model. There are clear differences between the whole-brain flexibility and the null distributions, but the flexibility values computed from null models, based only upon the number and size of communities, remain strong predictors of a subject's whole-brain flexibility.

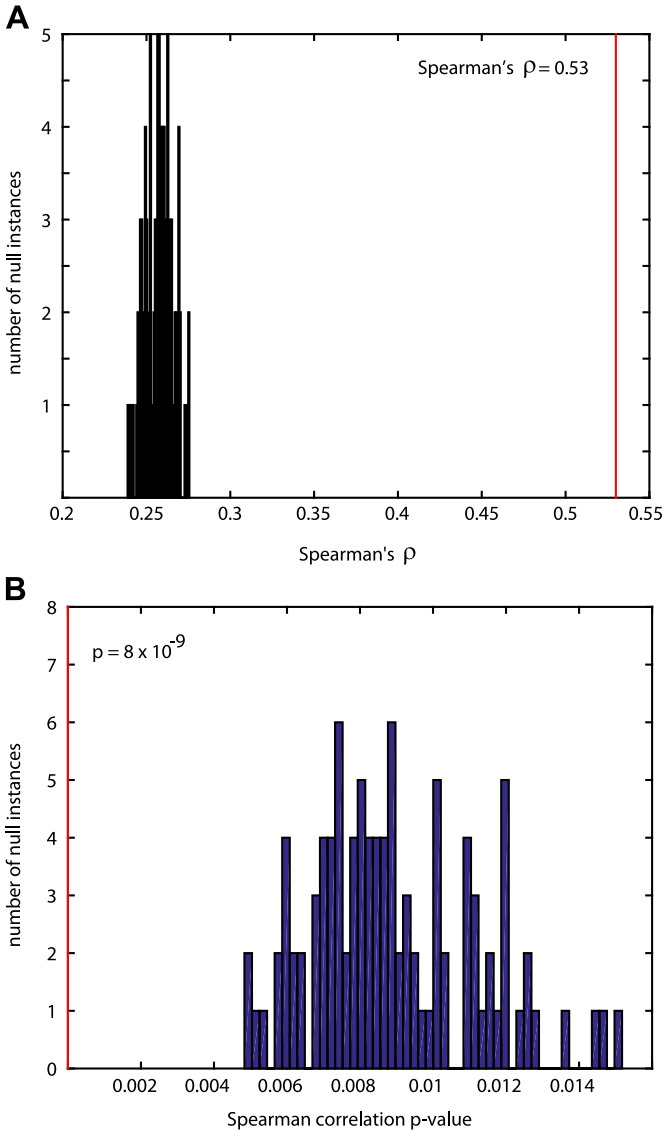

Fig. 10. Age-flexibility relationship in functional brain networks and null models. A: The solid red line shows the Spearman correlation value between whole-brain flexibility and age; the bars show a histogram of the same Spearman correlation values, each computed from one set of 100 community-number-preserving null models. B: The solid red line shows the *p*-value of the Spearman correlation observed in the data; the bars show the null distribution of *p*-values corresponding to the null Spearman correlation values in A. While all null correlations between age and flexibility in shuffled community structures are fairly strong and statistically significant, all are quite distant from and weaker than the correlation between age and whole-brain flexibility, indicating that the number of communities alone cannot explain the entire correspondence between flexibility and age.

shift score – as predictors. We also include mean relative motion as a predictor, to ensure it is accounted for as in previous analyses. To test the significance of the fit, we use a permutation null model in which we shuffle the d-prime and criterion shift scores uniformly at random (separately for each measure), perform the fit again 1000 times, and compare the original beta value for each node to the null distribution of beta values produced by these fits to permuted data. When uncorrected for multiple comparisons, 20 non-zero d-prime beta values and 20 non-zero criterion shift score beta values are significantly different from random (pi0.05). After a false discovery rate correction for multiple comparisons, only a single beta, with an original fit value of zero, is significantly different from its null distribution. This suggests that there is no significant correspondence between the performance measures from this task and the brain metrics we investigate here, even on a node-by-node basis.

To test the possibility that interactions between age and task performance are predictive of neural dynamics measures, we performed a multiple regression analysis including the effects of age, d-prime and criterion shift scores, as well as the interaction between age and each of the two performance scores. We also included mean relative motion as a predictor to ensure it was accounted for. However, we found that none of the interaction terms between age and performance – nor, indeed, any other terms save age itself and mean relative motion – had any significant influence on flexibility, number of communities, or recruitment.

3.3.1. Interdependence of community measures

We observe a very strong correlation between the number of communities in a subject's brain network and that subject's whole-brain flexibility (Pearson's r=0.65, $p < 0.001$). The correspondences with age for number of communities and flexibility are likely also related and may in fact be different measures of what is fundamentally the same phenomenon. For example, consider two separate communities in an older subject, which still have mutually coherent activity and recruit from the same set of brain regions. These brain regions may flexibly switch allegiances between the two communities during the experiment if they could be nearly equally well associated with either community. However, in a younger subject with stronger overall functional associations, these regions would be more likely to all be grouped into a single community throughout the experiment, and thus display far lower flexibility, stemming from the smaller community number.

To understand the dependence of flexibility on community number, we construct a null model in which we shuffle the community assignments of nodes in each subject's brain network uniformly at random. This preserves the number and size of communities in each brain network while destroying other structure that may be contributing to the flexibility. We re-compute flexibility in each of 100 null-model community structures for each subject.

We consider a null model in which community assignments were randomized individually within each time window of each subject's network. This destroys spatial/topological community structure as well as the continuity of communities over time. Fig. 9 shows the whole-brain flexibility of each subject (ordered) as well as the corresponding

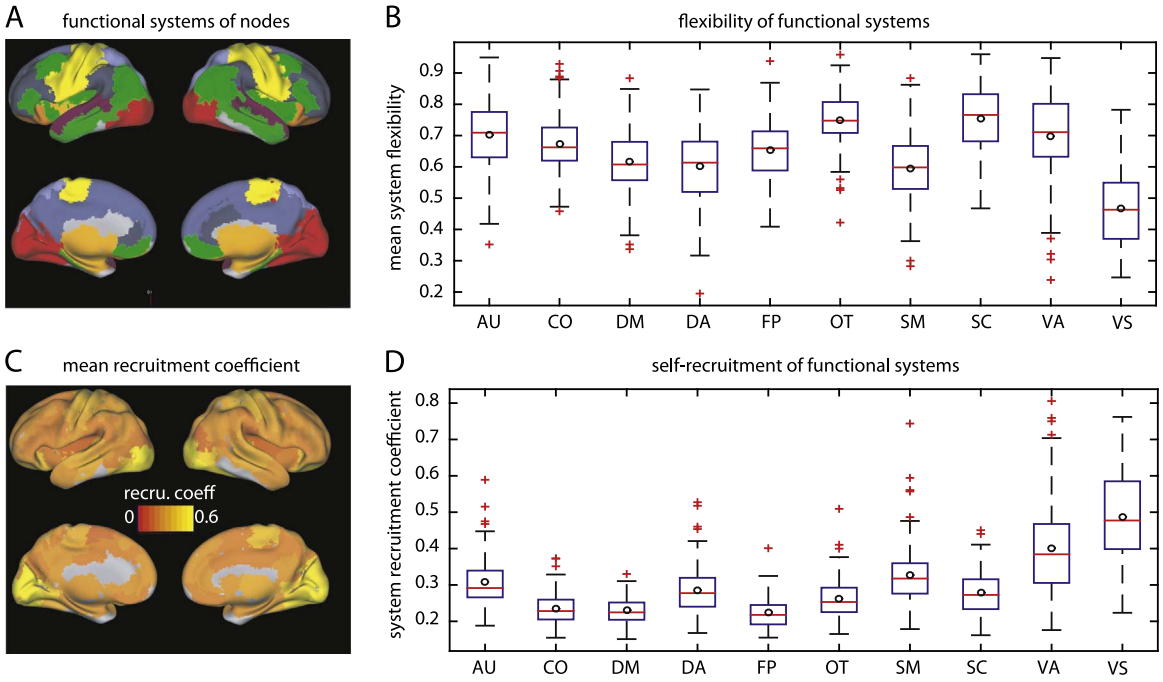

Fig. 11. Community organization of functional systems. A: The functional system partition of brain regions, with systems indicated by color. Systems identified (in color order from purple to red) are auditory (AU), cingulo-opercular (CO), default mode (DM), dorsal attention (DA), fronto-parietal (FP), other (OT), somatosensory (SM), subcortical (SC), ventral attention (VA), and visual (VS). B: Box plot showing the mean flexibility of brain regions in each functional system, and the distribution of this mean flexibility over subjects. C: Recruitment coefficients of each brain region (network node); visual cortex and somatosensory regions in particular have exceptionally high recruitment. D: Box plot showing the self-recruitment of each functional system, and its distribution over subjects.

null distribution of flexibilities for 100 community-number-preserving randomized community structures for the same subject. Clearly, preserving the mere number of communities separately in each network time window produces much higher flexibilities for all subjects, and does so very consistently, with a low variance among the 100 random instance of the network. Indeed, there are much greater differences in null flexibility across subjects than across random instances within a single subject.

When community structure information other than the number and size of communities is destroyed, we still see significant correlations between subject age and the flexibility computed from the shuffled community structure. However, these null-model correspondences are notably less strong than the correlation between age and flexibility, which contains information on flexibility beyond that explained by mere community number and size distributions (Fig. 10).

Although the measure of flexibility is not completely explained by community number in this case, there is still a clear and strong correlation between a subject's whole-brain flexibility and the mean flexibility of regions in the corresponding null model (Pearson's $r = 0.76$, $p < 0.001$). This indicates that the information contained in community size and number distributions alone does predict relative subject flexibility quite well.

3.4. Community organization and functional circuits

Having examined the dynamic community structure of individual functional networks largely on its own, in a data-driven manner, we aim to further understand and quantify how this structure corresponds to known functional systems in the brain. Fig. 11 shows the locations (A) and flexibilities (B) of the ten functional systems considered: auditory (AU), cingulo-opercular (CO), default mode (DM), dorsal attention (DA), fronto-parietal (FP), other (OT), somatosensory (SM), subcortical (SC), ventral attention (VA), and visual (VS). Consistent with Fig. 5A, the visual system is the least flexible, followed by the somatosensory. The high inter-subject variance in ventral attention regions likely reflects the relatively small size of that system (4 brain regions) (12).

In addition to total community number and whole-brain flexibility, we examine whether the relationships between community structure and age differ across these specific functional systems, as visualized in Fig. 11A and described in Methods. We find that the number of distinct communities into which regions of each individual functional system are grouped is significantly positively correlated with age, for all ten functional systems. Mean flexibility and age are positively correlated in all ten functional systems, with all correlations significant ($p < 0.05$) except in the visual system. The visual regions have the lowest mean flexibility overall (Fig. 11B) and the highest variance in flexibility across subjects. However, when mean relative motion is partialed out of the correlation, they also have the weakest relationship between system-wide flexibility and age.

We further examine the correspondence between functional communities and known functional systems using the *recruitment coefficient*, a measure of how cohesively regions from the same functional system are grouped together. Fig. 11C shows the recruitment coefficient of each region (Eq. (3)), and Fig. 11D shows the self-recruitment of each entire system (Eq. (4)). Again consistent with our flexibility findings, as well as previous reports of recruitment in the literature (Bassett et al., 2014), the visual and somatosensory systems have the highest self-recruitment, indicating that they are the systems most consistently grouped together in communities across time windows.

Whole-brain recruitment, or the average of region recruitment over all brain regions, is significantly anticorrelated with subject age (Spearman's $\rho = -0.32$, $p < 0.05$), as shown in Fig. 12. However, we find that system-specific self-recruitment is affected differently by age in different circuits. System recruitment is significantly anticorrelated with age only in cingulo-opercular, somatosensory, subcortical, and ventral attention regions, but no correlation is apparent in other regions, such as the visual system (see Figs. 13 and 14).

3.4.1. Dependence of recruitment on community size distributions

To ensure that the recruitment values reported here are not driven primarily by the size and number of communities detected, we again use a null model that permutes the community assignments of nodes

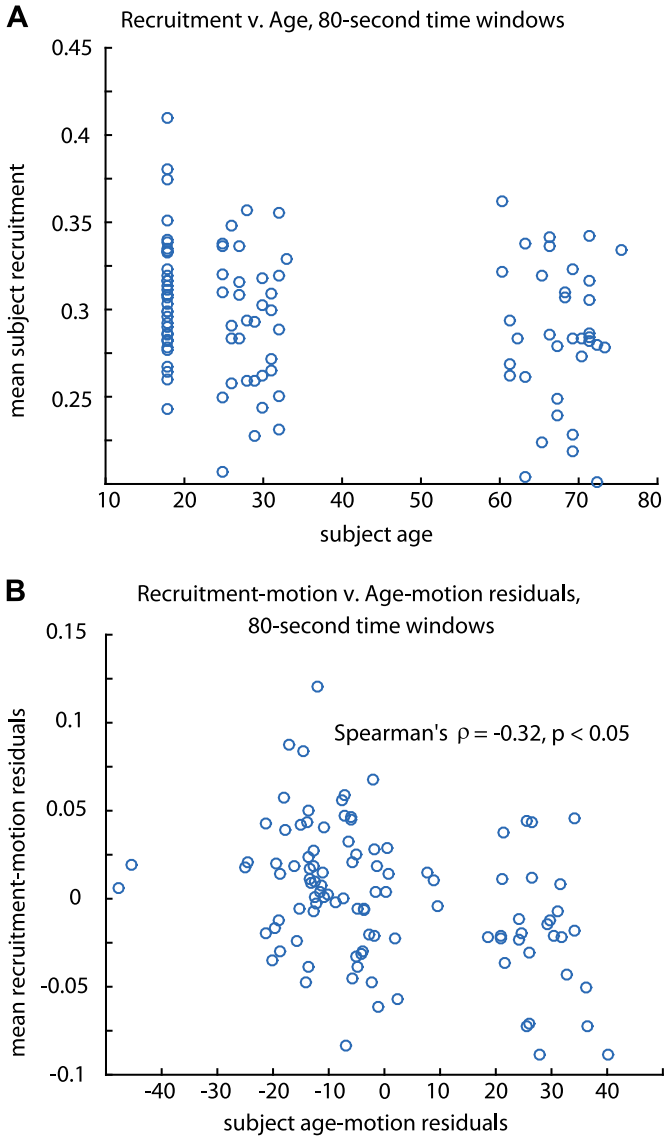

Fig. 12. Brain region recruitment and age. A: Scatter plot of the correspondence between subject age and average recruitment across all brain regions in networks with 80-s time windows. B: Scatter plot showing the significant negative correlation between these measures with mean relative motion partialed out.

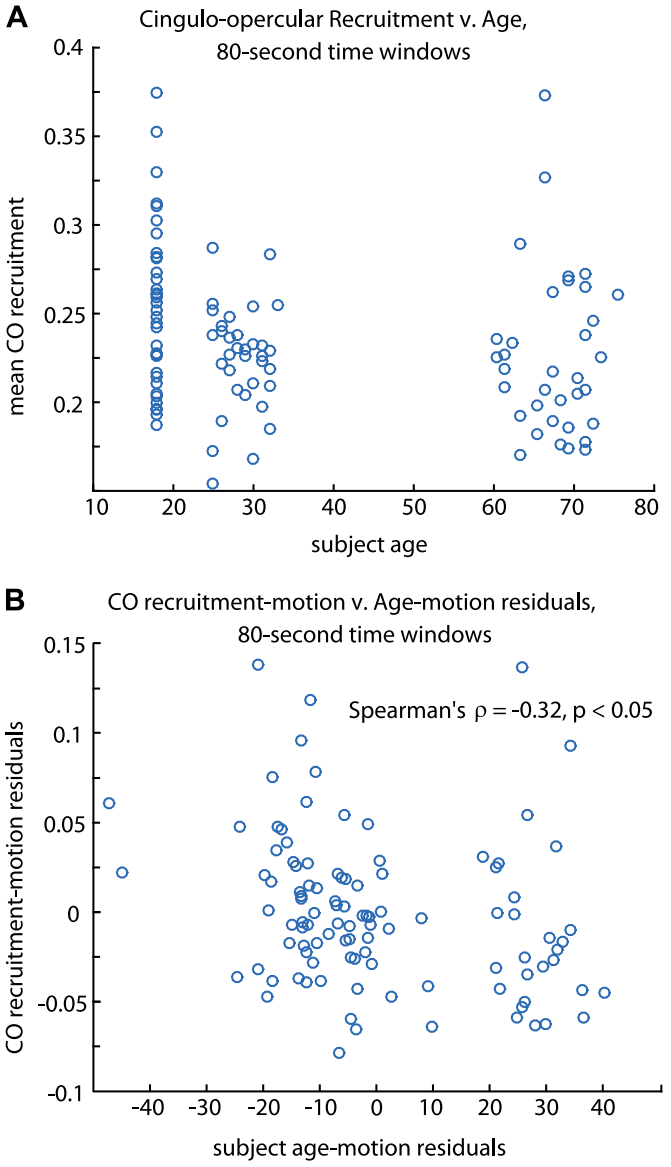

Fig. 13. System self-recruitment and age. A: Scatter plot of the correspondence between cingulo-opercular system self-recruitment and subject age in networks with 80-s time windows. B: Scatter plot showing a significant anticorrelation between these measures with mean relative motion partialed out (plot shows residuals of separately regressing each measure on mean relative motion). C: Scatter plot of the correspondence between visual system self-recruitment and subject age in networks with 80-s time windows. D: Scatter plot of the correspondence between visual self-recruitment and age with mean relative motion partialed out; there is no apparent correlation.

within each subject's network uniformly at random, but preserves community size and number distributions as well as time continuity. We compute the mean recruitment over all nodes in each subject's brain in each of these random null networks, as well as the recruitment of each functional node system. Fig. 15 summarizes the results. All subjects have mean whole-brain recruitment values significantly higher than those expected from networks with identical community size distributions but no other structure, indicating that the association of algorithmically identified communities with known functional systems is significantly greater than random. Within individual functional systems, results vary. Some systems, including sensory and motor cortices (auditory, somatosensory, and visual) and subcortical structures, are consistently associated with identified communities at a rate significantly greater than random. Others, including systems identified with executive control, both focused and bottom-up attention, and the resting state, have recruitment values that could reasonably be explained by chance in several subjects (i.e., similar values were found in randomized community structures that share only community size and number distributions with the corresponding human brain community structures).

4. Discussion

These findings relating functional community dynamics to age provide important insight into factors affecting the significant individual differences in community dynamics. The community structure appears to act as a signature of individual functional dynamics that is strongly influenced by age, indicating that cognitive organization during such a memory task differs across the lifespan of participants.

Interestingly, despite marked differences in community dynamics, we find no significant correspondence between community structure measures and performance on the memory task, and no age-related differences in memory performance or strategy were detected in this experiment. This is likely related to the choice to study only healthy adults with no measured deficits in cognitive function. It may also be partly explained by the timescales which we are able to probe; if criterion shift score and task accuracy are related to changes in brain

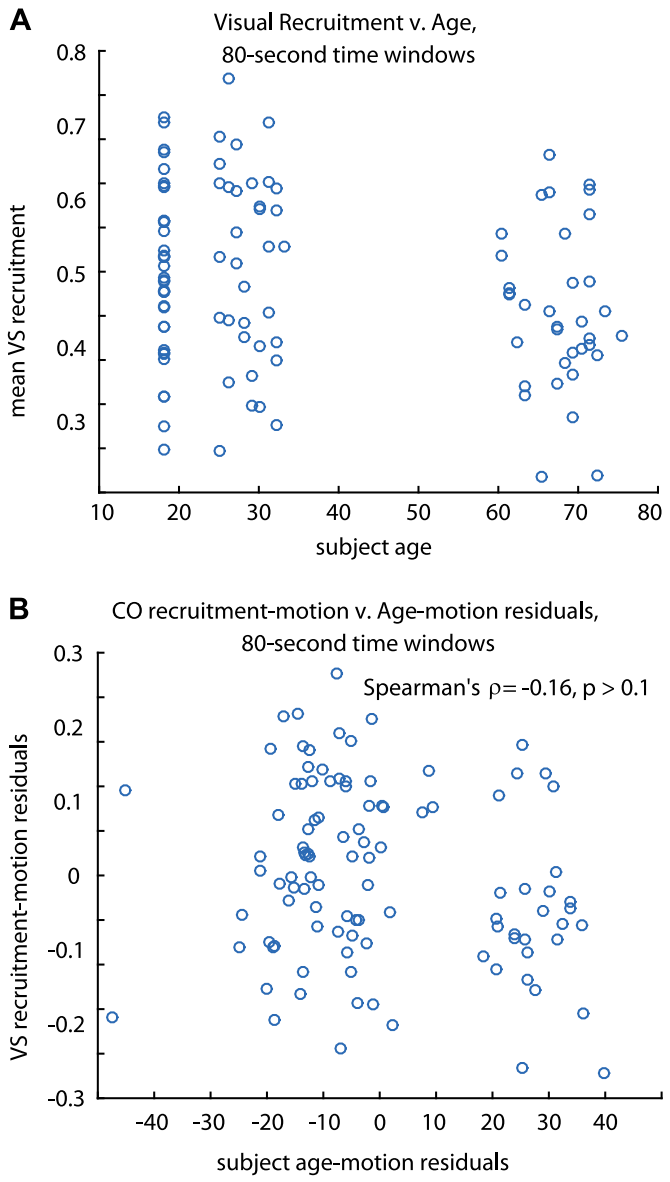

Fig. 14. System self-recruitment and age. A: Scatter plot of the correspondence between visual system self-recruitment and subject age in networks with 80-s time windows. B: Scatter plot of the correspondence between visual self-recruitment and age with mean relative motion partialed out; there is no apparent correlation.

dynamics primarily at the level of single trials or strategy blocks, these changes may be somewhat obscured in our dynamic networks. However, it is clear that the dynamic community structure delineated by the slower fluctuations – e.g., in phasic arousal, attention, or strategy – do show significant changes related to demographics, to which our analyses are sensitive. Future studies designed to elicit greater performance differences, either by increasing task difficulty or by including a population of individuals with age-related cognitive impairment, could probe whether individual patterns of community dynamics are associated with these age-related changes in memory ability, and determine which dynamics at which timescales correspond to retention or deterioration of performance.

We found that age correlates positively with community number and flexibility. That is, older adults tend to have more fragmented communities with less coherent activity than those in younger adults. Furthermore, brain regions are more likely to switch their community membership in older adults, a result only partially explained by the existence of more communities to switch between. Taken together, these results agree with previous findings from task-free paradigms, insofar as the brains of older adults tend to show a loss of the within-network integrity that might have led to them being grouped in fewer and larger coherent communities, while at the same time losing segregation between communities and seeing more fluidity of community membership over the course of the memory task.

Using null models, we show that the overall connectivity, or density, of a subject's brain network has some influence on the number of communities detected, and hence also on the flexibility. This may be related to the resolution limit inherent in modularity maximization algorithms for community detection, in which the network density determines an intrinsic scale to the modularity that prevents the detection of communities below a certain size (Fortunato and Barthelemy, 2007). In multi-slice modularity maximization in general, the addition of links (here of weight ω) to connect communities across network slices affects the resolution limit of the problem, potentially biasing the number of communities as well as the flexibility. This complicated interaction between the time resolution parameter and overall network connectivity makes the mechanism underlying the changes in flexibility and community number more difficult to isolate. Here we have employed null models to probe the extent of the influence of OC on our results; however, future work is needed to fully elucidate this relationship.

We also investigate the correspondence of communities to known functional systems in the brain, and find that this correspondence is modulated by age in several circuits involved in cognitive control, including ventral attention, cingulo-opercular, and subcortical systems. The ventral attention system is involved in bottom-up attention, or response to infrequent or unexpected cues (Vossel et al., 2014). The cingulo-opercular circuit, composed of anterior cingulate cortex as well as the supramarginal gyrus, rostral middle frontal gyrus, and sections of inferior frontal gyrus, is thought to underlie tonic alertness and the maintenance of available function during a task, and to be important for cognitive control during working memory (Cohen et al., 2014; Sadaghlani and D'Esposito, 2015). The cingulo-opercular functions also include contribution from thalamus, which is categorized as a subcortical region in this scheme. The subcortical regions are less finely divided than the cortical regions in this atlas, so the subcortical nodes have larger volume and are more functionally heterogeneous (Hagmann et al., 2008). Thus, the results involving subcortical regions likely contain less information on meaningful functional correlations than results involving cortex, since the signal from these regions is averaged over a larger area containing distinct functional responses.

Overall, these results show that age-related differences are evident during the memory task in specific circuits related to attention and cognitive control (as well as the task-related somatosensory network), which is consistent with past findings that cognitive control is modulated by age (Cepeda et al., 2001; West et al., 2002; Treitz et al., 2007). The relationship between regions identified as theoretically meaningful on the basis of prior GLM-based analyses of BOLD activity, and the sort of dynamic, system-level connectivity of interest here, is not yet well understood. However, this study demonstrates that we can use a data-driven method to discover regions of interest for aging and task function about which it is still very difficult to make *a priori* hypotheses at this scale, based on our previous understanding of the neural processes involved in this task. The results of this and other similar investigations can be used to guide further study with different methodologies, and provide a valuable complementary body of knowledge to that gleaned from traditional, more static methods of analyzing BOLD activity.

The finding that age selectively modulates the cohesive functional grouping of these cognitive control circuits, as well as the task-involved somatosensory cortex, shows that specific cognitive systems differ notably across the lifespan, while others remain relatively unaffected by age. Importantly, although we can identify the extent of each circuit's functional changes across the lifespan, the behavioral effects of differences in these circuits remain unclear. All participants in the

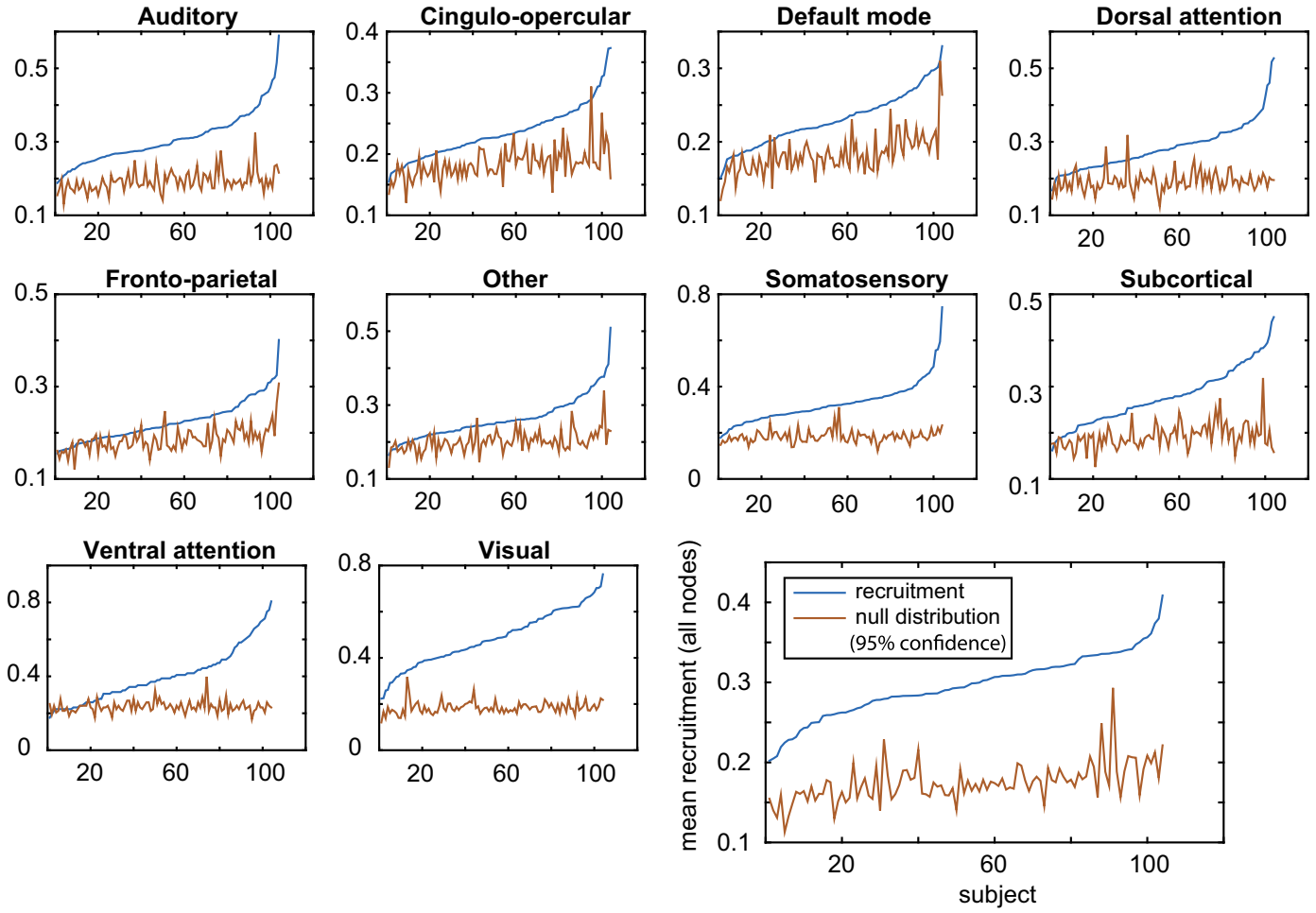

Fig. 15. Dependence of recruitment on community size distributions. Bottom right: Recruitment values for each subject (blue line), averaged over all brain regions, alongside 95% confidence line (red line) from null distribution of 100 recruitment values computed in community-size-preserving null networks. All subjects have mean whole-brain recruitment values significantly higher than those expected in null networks, indicating that the association of algorithmically identified communities with known functional systems is statistically significant. Smaller panels: Recruitment values for each subject (blue lines), averaged over brain regions in known functional systems, alongside 95% confidence lines (red lines). Some individual systems, including sensory and motor cortices (auditory, somatosensory, and visual) and subcortical structures, are consistently associated with identified communities at a statistically significant rate. Others–including systems identified with executive control, both focused and bottom-up attention, and the resting state–have recruitment values that could reasonably be explained by chance in several subjects.

experiment were cognitively healthy and none showed memory impairment; furthermore, no age-related differences in performance were evident despite the clear changes we observed in functional organization. The presence of such widespread neural changes, with no manifest change in behavior, strongly suggests that compensatory mechanisms may be playing a role in this cognitive task for older adults, as proposed in previous work (Cabeza et al., 2002; Grady, 2008). While this study cannot identify which age-related changes are beneficial to memory performance rather than detrimental, the methods used here provide a framework for quantifying such changes in community structure and dynamics, in future studies where age-related performance differences are evident.

5. Conclusion

Overall, this work confirms that the dynamics of functional community structure in the human brain during a memory task vary considerably with age. In particular, both whole-brain flexibility, which measures the tendency of brain regions to switch between communities over time, and the overall number of functional communities show notable individual differences and are strongly correlated with age, with older subjects demonstrating significantly higher flexibility and more fragmented functional communities. Using quantitative methods of comparing the community structure to known functional brain systems, we also examine the tendency of brain systems to be grouped cohesively together in communities during the memory task. We find that this tendency is significantly modulated by age in brain regions associated with cingulo-opercular, somatosensory, ventral attention, and subcortical circuits, but not in other brain areas. These results identify age as an important driver of individual variation in functional community dynamics, and provide insight into how aging differentially impacts the functional organization of different brain systems, even in healthy adults who do not experience declines in performance. Additionally, they demonstrate methods which promise to be useful in quantifying which circuits drive changes in network organization across a broad range of situations, including in task-active networks.

Acknowledgements

This work was supported by the National Science Foundation Graduate Research Fellowship under grant DGE-1144085, the Packard Foundation, and the Institute for Collaborative Biotechnologies through grant W911NF-09-0001 from the U.S. Army Research Office. The content of the information does not necessarily reflect the position or the policy of the Government, and no official endorsement should be inferred.

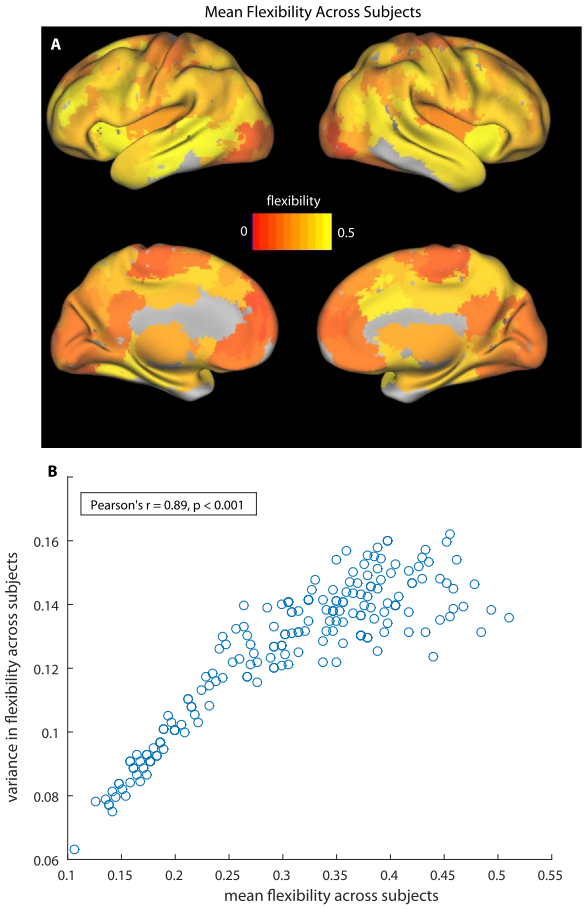

Fig. A1. A: Flexibility of the 194 brain regions used as network nodes in networks with 500-s time windows. Color indicates mean flexibility over N=104 subjects. Visual cortex and somatosensory regions in particular have exceptionally low mean flexibility, as also observed with 80-s time windows. B: Scatter plot of mean region flexibility against variance in region flexibility across subjects. Brain regions that are more flexible on average have a strong tendency to also display higher cross-subject variance in flexibility. This is the opposite effect from that seen in networks with 80-s time windows (Fig. 5 in the main manuscript), due largely to the much higher cross-subject variability seen in high-flexibility (non-motor, non-visual) regions with 500-s time windows.

Appendix A. Appendix

In this Appendix, we present the following information:
1. dynamic community structure results in dynamic functional networks with 500-s time windows;
2.1. details on the choices of spatial and temporal resolution parameters for the community detection algorithm;
2.2. details on categorical versus time-ordered definitions of flexibility;
2.3. an analysis of single-node communities, or “singletons”, and results when they are excluded from the analysis;
2.4. discussion of behavioral and brain-measures outliers and their e ect on the results;
2.5. details and discussion of the statistical correction for mean relative motion.

A.1. Results from networks with 500-s time windows

Here we present further results from networks with 500-s time windows, which capture dynamics associated with a much longer time scale than the 80-s time windows that are the focus of the main manuscript. Overall, these results are mostly qualitatively similar to those found for 80-s time windows, but the correlations between demographics or performance measures and brain community structure measures are weaker.

A.1.1. Brain region flexibility

As discussed in the main manuscript, we find that in networks with 80-s time windows, highly flexible brain regions are very consistently flexible across subjects, while those with lower mean flexibility show greater inter-subject variance in flexibility. On longer timescales, in networks with 500-s time windows, the identities of the brain regions with the lowest mean flexibility – i.e., regions in visual and motor cortex – are largely the same as those found with 80-s time windows (Fig. A1A), and their cross-subject variance is quantitatively similar as well. However, the regions with higher mean flexibility – i.e., non-visual and non-motor regions – are much more variable in flexibility across subjects in networks composed of 500-s time windows. This leads to a strong correlation between mean flexibility and cross-subject variance with 500-s time windows, shown in Fig. A1B, whereas 80-s time windows lead to a similarly strong anticorrelation (as shown in Fig. 5 in the main manuscript).

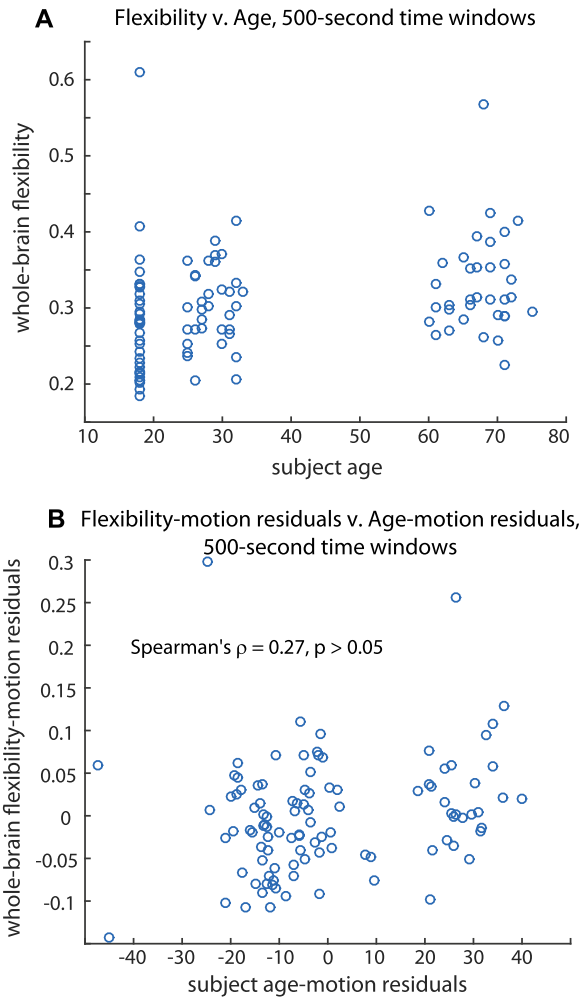

Fig. A2. A: Scatter plot of the uncorrected correspondence between subject age and whole-brain flexibility in networks with 500-s time windows. B: Scatter plot showing residuals of separately regressing each measure on mean relative motion. The correlation between these residuals is not significant, indicating that there is no significant relationship between age and flexibility in these networks that cannot be explained by mean relative motion.

The cohesive dynamics of visual and motor systems thus show similar flexibility patterns across subjects even on very different timescales, while individual differences in the dynamics of other brain regions are more strongly impacted by the choice of time resolution. This may be because visual and motor components of the memory task do not differ across trials, leading to strong functional similarity throughout the entire experiment.

A.1.2. Whole-brain flexibility, number of communities, and recruitment

The strong correspondence between age and whole-brain flexibility seen with 80-s time windows, and presented in the main manuscript, is not statistically significant in networks with 500-s time windows (Fig. A2). This indicates that the community dynamics modulated by age here are relevant on shorter timescales of only a few minutes, which correspond more closely to the timescales of cognitive function demanded by the task setup.

With 500-s time windows, there is also no significant correspondence between dynamic community number and age, and the number of distinct communities in individual functional systems is significantly positively correlated with age only in four systems: auditory, somatosensory, subcortical, and ventral attention. The weakening of both the age-flexibility correspondence and the age-community number correspondence on this longer timescale is consistent with the possibility that flexibility and community number are related.

The correspondence between subject age and the mean recruitment coefficient over all brain regions is shown in Fig. A3. There is a highly significant anticorrelation between these measures (Spearman's $\rho = -0.42$, $p < 0.001$) with both 500-s and 80-s time windows.

A.1.3. System-specific recruitment

In networks with 500-s time windows, system-specific recruitment is significantly anticorrelated with age only in cingulo-opercular (Fig. A4), subcortical, ventral attention, and auditory systems, but not in other systems (such as the visual system, shown in Fig. A5). This effect is consistent across timescales for cingulo-opercular, subcortical, and ventral attention regions.

A.2. Methodological details and considerations

A.2.1. Resolution parameters

The spatial resolution parameter γ determines the relative weight given to the randomized null model as compared to the data in each time

Fig. A3. A: Scatter plot of the uncorrected correspondence between subject age and average recruitment across all brain regions in networks with 500-s time windows. B: Scatter plot showing the significant negative correlation between these measures with mean relative motion partialed out. Older subjects have significantly lower recruitment on average over brain regions than younger subjects on both timescales investigated.

window when finding a partition. Varying γ changes the number and size of communities found in the partition – higher values of γ favor many small communities, while lower values favor fewer, larger communities. In order to choose a spatial resolution that will give meaningful results about brain organization on the scale of our chosen atlas, we prefer γ values at which the stochastic algorithm tends to produce less variation in partitions across algorithm runs. We measure variation among partitions with the z-score of the Rand coefficient, which measures the extent to which two partitions are similar compared to the expected similarity of randomized partitions Traud et al. (2011), averaged over all pairs of partitions produced by the algorithm. It has been shown in simulated networks of oscillators that the lowest cross-subject variance in Rand z-score occurs at the value of γ that produces communities corresponding to the size and number of "ground-truth" communities in the network Bassett et al. (2013). However, since human brain functional networks have meaningful activity at various scales, we see no clear maximum in Rand z-score corresponding to a minimum in Rand z-score variance at any single value of γ. In networks with 80-s time windows, we choose $\gamma = 1.2$ – a value between $\gamma = 1$, which often gives just two or three large communities, and $\gamma = 1.4$, which in many subjects gives as many at 100 communities (more than half the total number of nodes) – in order to obtain communities that are on average similar to the size of the functional systems we are interested in. For 500-s time windows, we choose $\gamma = 1.15$ for the same reason. Both of these choices lie in a range of values over which Rand z-score and its variance are relatively uniform, indicating that the consistency of the communities detected does not depend sensitively upon this parameter. In addition, the Rand z-score is high for all choices, indicating that the community partitions detected are significantly more consistent across these parameter values than would be expected of community partitions with the same community size distributions selected at random.

The time resolution parameter ω determines the relative weight given to intra-window (non-temporal) and inter-window (temporal) considerations when finding a partition. Here, in order to most clearly resolve the differences in the flexibilities of different brain regions, we choose the value of ω that maximizes the variance in flexibility across nodes. This value is $\omega = 0.05$ for 80-s time windows, and $\omega = 0.001$ for 500-s time windows.

A.2.2. Categorical versus time-ordered flexibility

Eq. (2) in the main manuscript, reproduced here, defines the metric of flexibility for each brain region:

$$f(i) = \frac{1}{T(T-1)} \sum_{t \neq t'} [1 - \delta(g_{it}, g_{it'})].$$

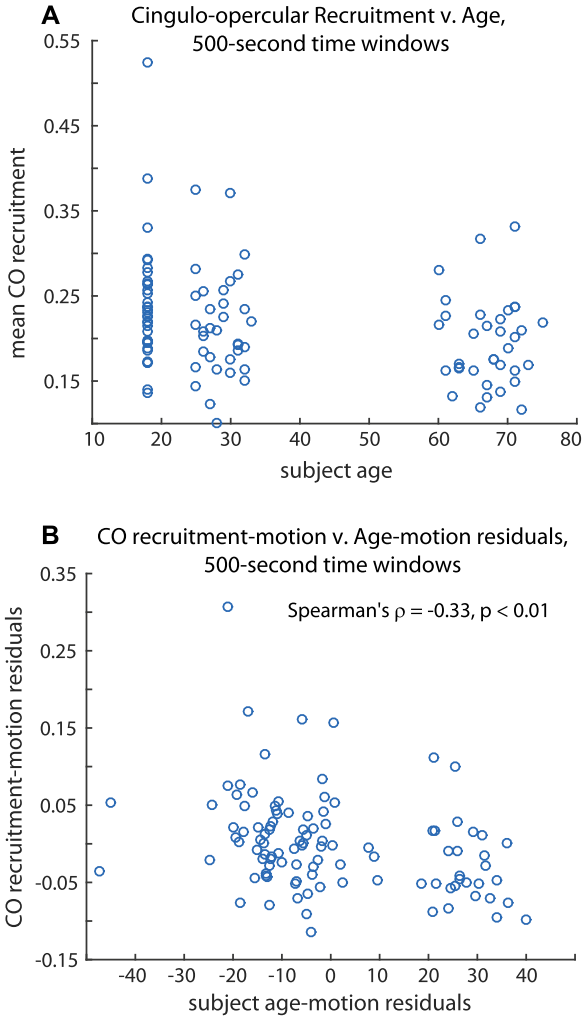

Fig. A4. A: Scatter plot of the uncorrected correspondence between cingulo-opercular system self-recruitment and subject age in networks with 500-s time windows. B: Scatter plot showing a significant anticorrelation between these measures with mean relative motion partialed out. Older subjects have significantly lower cingulo-opercular recruitment coefficients on both timescales investigated; this correspondence is also consistent across timescales in the subcortical and ventral attention systems. However, there are changes in the significance of this correspondence across timescales in some systems. In 500-s time window networks (unlike in 80-s time window networks), the recruitment-age correspondence is not significant in the somatosensory system, and it is significant in the auditory and default mode systems.

This method of calculating flexibility, known as "categorical" flexibility, compares the community assignments of nodes between all possible pairs of time windows, not just time-adjacent windows. Typical uses of categorical flexibility compare community assignments between categories or tasks without considering temporal changes. In this work, we use categorical flexibility to emphasize the consistency of nodes across long time windows. We choose to compare between all time windows equally (without imposing time order) since each window is long compared to the differing elements of the task on a trial or probability block level, and all windows are statistically identical with respect to task design (for 500-s windows) or nearly so (for 80-s windows). In this way we avoid assuming that changes in brain dynamics happen progressively over the course of the task, but instead focus on assessing stability of community structure over the entire task at once.

All results reported in the main manuscript use categorical flexibility. For comparison, we repeat our analysis using time-ordered flexibility:

$$f_{to}(i) = \frac{1}{T-1}\sum_{t=1}^{T-1}[1 - \delta(g_{it}, g_{i(t+1)})].$$

We find that the values of node flexibility and subject-wise whole brain flexibility are extremely closely correlated, as shown in Fig. A6. In addition, all correlations with categorical flexibility reported in the main manuscript are essentially unchanged when computed with time-ordered flexibility. This suggests that progressive changes in brain dynamics over the course of the task are less important at this time scale than overall consistency or variability of community assignments throughout the experiment, as we might expect with time windows representing multiple statistically similar portions of the same task.

A.2.3. Analysis of single-node communities

As seen in Fig. 4 in the main manuscript, the community detection algorithm identifies communities of size 1 in the brain networks of many subjects. As described in the main manuscript, we identify both "dynamic singletons," or single-node communities that contain only one brain region across all time windows, and "static singletons," or communities with a single brain region in one time window, regardless of whether that community also extends across multiple time windows.

We find that across all subjects, there is only a single dynamic singleton identified in our data. Static singletons are more numerous, but still

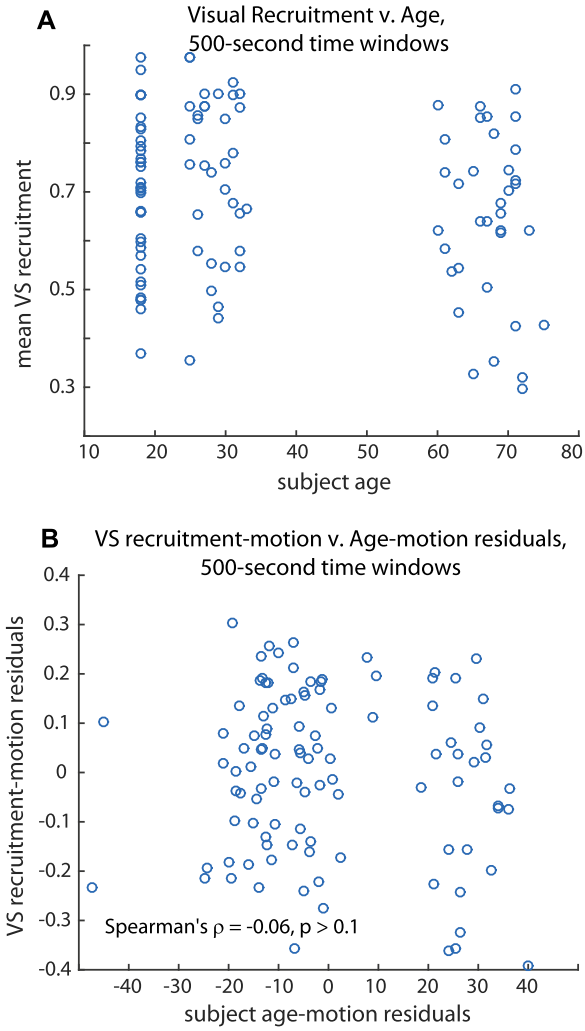

Fig. A5. A: Scatter plot of the correspondence between visual system self-recruitment and subject age in networks with 500-s time windows. B: Scatter plot of the correspondence between visual self-recruitment and age with mean relative motion partialed out; there is no apparent correlation on this coarser timescale, consistent with the result in 80-s time window networks.

remain sparse. Fig. A7 shows the number of communities identified in each time window for each subject with single-node communities excluded from each time window (cf. Fig. 3 in the main manuscript). These statistics appear qualitatively similar for almost all subjects.

A closer look at the cross-subject and cross-region distributions of static singletons is given in Fig. A8. Panel A shows the total number of static singletons (summed over 80-s time windows) in each subject and each brain region. Most static singletons to not tend to persist across time

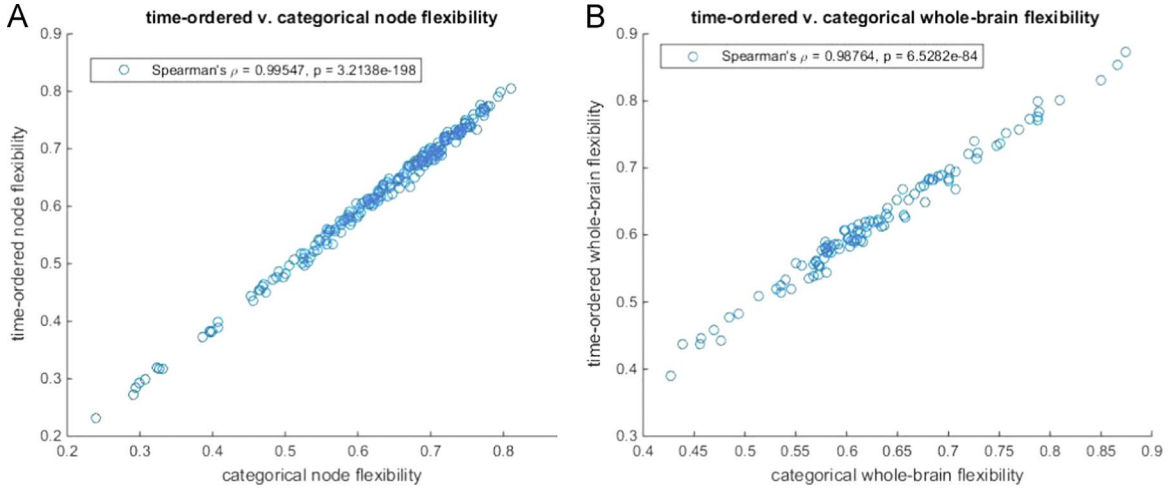

Fig. A6. Correspondence between categorical and time-ordered flexibility. A: Flexibility of each brain region (averaged over subjects). B: Whole-brain flexibility of each subject. Both measures show near-perfect correlation between categorical and time-ordered flexibility (Spearman's ρ=0.99, $p \approx 0$).

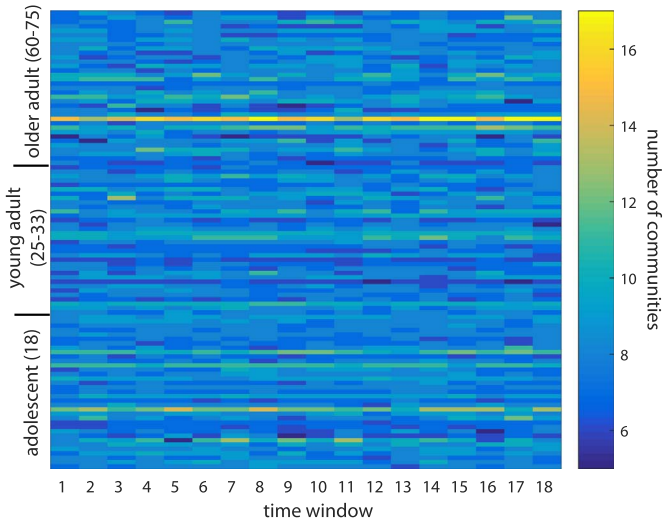

Fig. A7. Number of non-single-node communities. Color indicates the number of communities detected within each 80-s time window in each subject, excluding communities composed of only a single brain region within that time window. Subjects (on the vertical axis) are ordered by age. These results are qualitatively similar to the numbers of communities found in each subject with single-node communities included (see Fig. 3 in the main manuscript).

windows, either in particular subjects or in particular regions. However, one subject (subject 35) does have a handful of regions which are consistently singletons in 16 out of 18 time windows; this is very unusual and only occurs once in one other subject (subject 28). In panel B of Fig. A8 – which depicts the number of singletons by subject, with each color representing one brain region – the large contributions from these consistently single regions visibly boost the total singleton count for these two subjects, making them appear as outliers. (More details on outliers are given below.) Panels C and D both show the number of singletons for each brain region. In C, the colors represent the contributions from individual subjects, while in D, the colors represent contributions from the three age groups.

To ensure that singletons do not drive results, we repeat our analyses with these communities excluded from consideration. The correlation between age and number of communities, both overall and in specific functional systems, is nearly unchanged, as shown in Table A1. Although found in most subjects, static singletons are not significantly correlated with age and do not substantially affect age-related changes in community dynamics.

A.2.4. Analysis of outliers in task performance and brain measures

As noted in the main manuscript, two subjects appear to be bivariate behavioral outliers (see Fig. 2). In order to ensure that these anomalous performance values do not affect the behavioral correlations, we repeated our analysis with these two subjects removed. We had originally found no significant correlations, either between the d-prime and criterion shift performance measures, or between either of these measures and the brain measures of interest. With the outliers removed, we similarly find that all Pearson correlations between behavior measures and brain measures, as well as the correlation between d-prime and criterion shift, remain insignificant.

Similarly, two subjects in Fig. 3 in the main manuscript appear to have notably higher numbers of static communities than the rest. One of these subjects, subject 35, also has a notably higher number of static singletons, as seen in Fig. A8B, along with another subject who is not an outlier in number of non-singleton static communities. To ensure that these outliers are not driving results, we also repeat our analysis while excluding these three brain-measures outlier subjects. We find that the significance or non-significance of all correlations between brain measures (flexibility, number of communities, recruitment) and age or performance remain the same, both overall and in individual functional systems, with a single exception. That exception is the system-specific recruitment of the subcortical nodes, which is significantly correlated with age with the outliers included (Spearman's $\rho = -0.30$, $p = 2.33 \times 10^{-3}$, as reported in Table 1), but not once the outliers were removed (Spearman's $\rho = -0.26$, $p = 9.69 \times 10^{-3}$, which is not significant after correction for multiple comparisons).

A.2.5. Statistical correction for mean relative motion

As discussed in the main manuscript, since subject age is correlated with mean relative motion in these data, we expect motion to substantially affect the correspondence measures of community dynamics and age, and potentially other performance and demographic measures as well, due to the broad and non-uniform distribution of ages in our sample. Thus, all subject-wise correlations in this study are performed with mean relative subject motion partialed out – i.e., each correlation variable was first regressed separately on mean relative motion, and we assessed the correlation between the residuals of these regressions, to ascertain the extent of their relationship that could not be explained by motion. Some of the observed results are indeed affected by motion, showing a different level of correlation and significance with and without the motion correction. Here we report the differences we observe.

- The correlation between age and whole-brain flexibility is consistently highly significant both with ($r = 0.53$, $p < 0.001$) and without ($r = 0.40$, $p < 0.001$) motion correction in networks with 80-s time windows. Indeed, the correlation is stronger when motion is accounted for. However, in networks with 500-s time windows, a significant correlation ($r = 0.30$, $p < 0.05$) is observed only when not correcting for motion. When motion is accounted for, the correlation is weaker and does not pass the significance test.
- The correlation between age and number of communities evident in networks with 80-s time windows ($r = 0.29$, $p < 0.05$) is not significant without accounting for motion ($p > 0.1$). With 500-s time windows, there is no evident correlation between age and number of communities, and motion does not impact this result.
- The anticorrelation between age and average recruitment observed in networks with 80-s time windows ($r = -0.32$, $p < 0.05$) is not significant

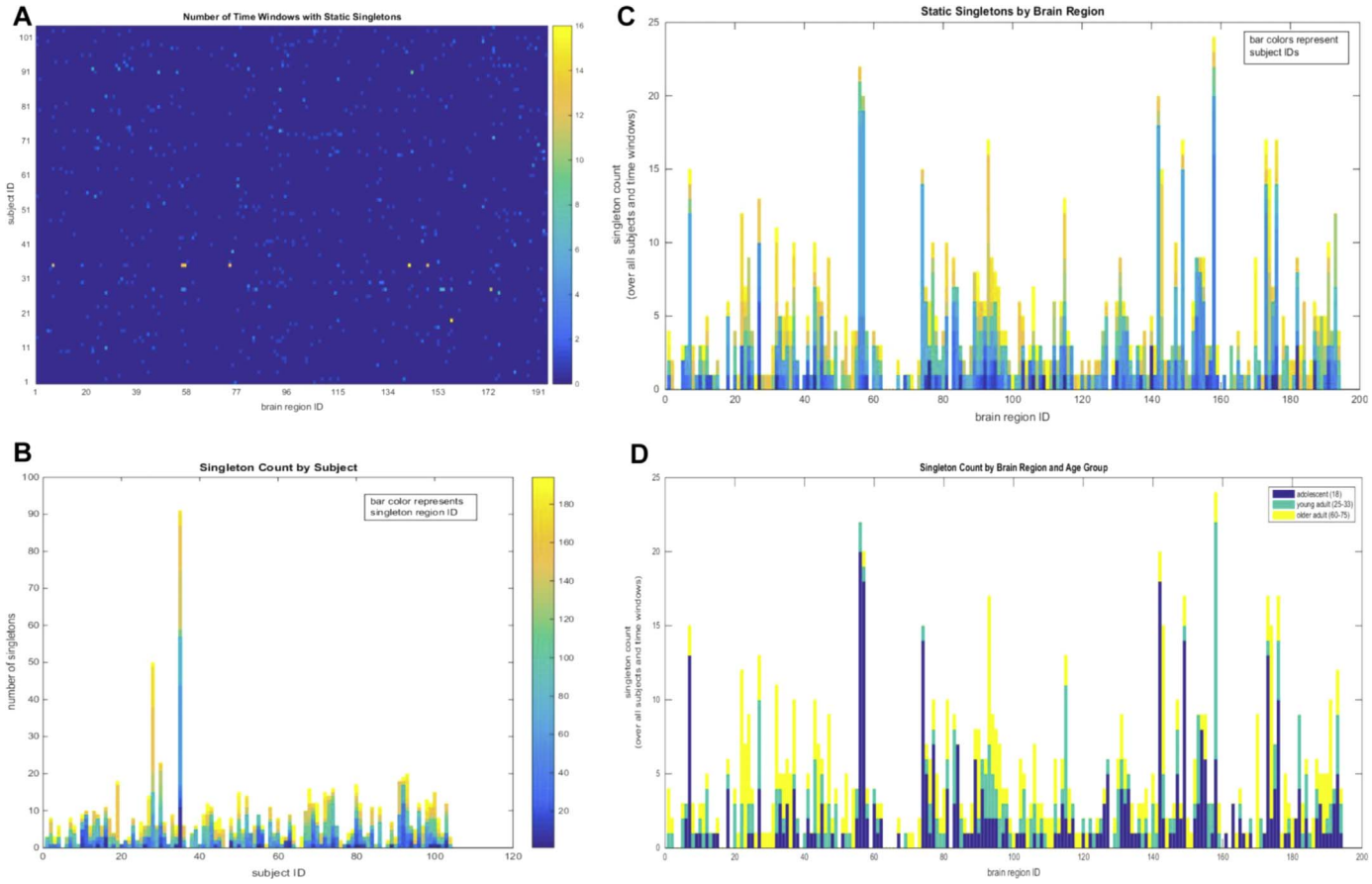

Fig. A8. A: Number of time windows in which each brain region is a static singleton in each subject. Static singletons are relatively sparse, and most regions are not consistently singletons across subjects or time windows. However, two subjects (subjects 28 and 35) have regions which are singletons in most of the 18 80-s time windows. B: Distribution of static singletons over subjects. Colors represent contributions from individual brain regions. Due largely to contributions from just one or two brain regions, subjects 28 and 35 have many more singletons than the others. C: Distribution of static singletons over brain regions. Colors here represent individual subjects. D: Distribution of static singletons over brain regions, as in C. Here, colors represent contributions from one of the three age groups.

without accounting for motion ($p > 0.1$). Similarly, the anticorrelation between age and average recruitment with 500-s time windows is only significant when motion is accounted for.

- Mean relative motion affects the correspondence between system-specific flexibility and age in several systems. Flexibility over 80-s time windows in the dorsal attention, subcortical, and ventral attention systems shows no significant correlation with age when motion is not partialed out, but does correlate with age when motion is accounted for. On the other hand, flexibility over 80-s time windows in the visual system does not correlate with age when motion is accounted for, but correlates only when motion is not partialed out. The correlation between age and system-specific flexibility over 500-s time windows is not affected by this motion correction in any specific systems.

Table A1
Correlations between subject age and number of non-singleton communities. Spearman rank correlation ρ values and associated p-values for correlations between age and community number, with single-node communities excluded. Mean relative motion has been partialed out of all correlations. All correlations are statistically significant ($p < 0.05$) after family-wise error rate correction for multiple comparisons, and values are essentially unchanged from corresponding values with single-node communities included.

	Age v. Community Number	
	(single-node communities excluded)	
	Spearman's ρ	p-value
Whole brain	0.28852	0.0031207
Auditory	0.38723	5.33E-05
Cingulo-opercular	0.36970	1.21E-04
Default Mode	0.40874	1.82E-05
Dorsal Attention	0.34042	4.34E-04
Fronto-parietal	0.33858	4.68E-04
Other	0.35313	2.53E-04
Somatosensory	0.40325	2.41E-05
Subcortical	0.38999	4.66E-05
Ventral Attention	0.39083	4.47E-05
Visual	0.37777	8.36E-05

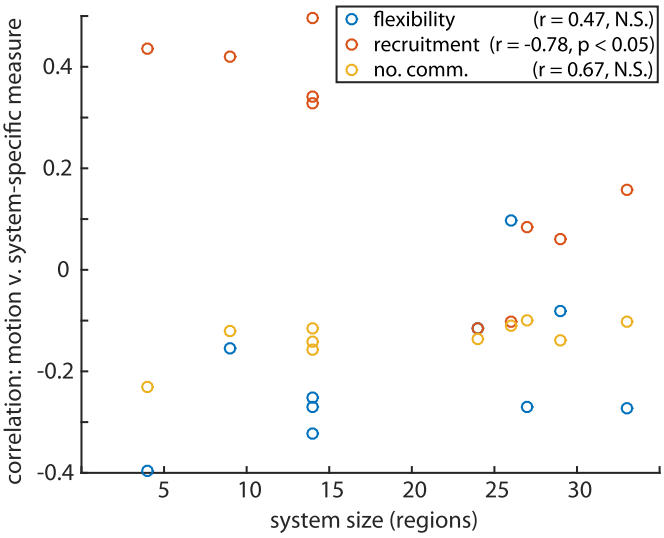

Fig. A9. Scatter plot of the correspondence between functional system size and the effect of motion on system-specific community structure diagnostics. System size reliably predicts the strength with which motion will correlate with system self-recruitment, but this effect is not observed for other diagnostics, such as system flexibility or number of communities in a system.

- Motion also affects system-specific recruitment and its correlation with age. When motion is not accounted for in 80-s time window networks, none of the functional systems have self-recruitments that significantly correlate with age. When motion is not accounted for in 500-s time window networks, three systems show a significant anticorrelation between self-recruitment and age: cingulo-opercular and subcortical, which show the same results with motion partialed out, and fronto-parietal, which does not.
- Overall, we find that mean relative motion is most likely to affect recruitment in small systems (i.e., those composed of fewer brain regions). This is depicted in Fig. A9, which shows a significant correlation between system size and the strength of the correlation between motion and system self-recruitment. However, we do not see a similar relationship between system size and the effect of mean relative motion on system flexibility or number of communities in the system.

References

Aminoff, E.M., Clewett, D., Freeman, S., Frithsen, A., Tipper, C., Johnson, A., Grafton, S.T., Miller, M.B., 2012. Individual differences in shifting decision criterion: a recognition memory study. Mem. Cogn. 40, 1016–1030.

Aminoff, E., Freeman, S., Clewett, D., Tipper, C., Frithsen, A., Johnson, A., Grafton, S., Miller, M., 2015. Maintaining a cautious state of mind during a recognition test: a large-scale fmri study. Neuropsychologia 67, 132–147.

Balota, D.A., Dolan, P.O., Duchek, J.M., 2000. Memory changes in healthy older adults. In: The Oxford Handbook of Memory. pp. 395–409.

Bassett, D.S., Bullmore, E.T., Meyer-Lindenberg, A., Apud, J.A., Weinberger, D.R., Coppola, R., 2009. Cognitive fitness of cost-efficient brain functional networks. Proc. Natl. Acad. Sci. 106, 11747–11752.

Bassett, D.S., Wymbs, N.F., Porter, M.A., Mucha, P.J., Carlson, J.M., Grafton, S.T., 2011. Dynamic reconfiguration of human brain networks during learning. Proc. Natl. Acad. Sci. 108, 7641–7646.

Bassett, D.S., Nelson, B.G., Mueller, B.A., Camchong, J., Lim, K.O., 2012. Altered resting state complexity in schizophrenia. NeuroImage 59, 2196–2207.

Bassett, D.S., Porter, M.A., Wymbs, N.F., Grafton, S.T., Carlson, J.M., Mucha, P.J., 2013. Robust detection of dynamic community structure in networks. Chaos 23, 013142.

Bassett, D.S., Yang, M., Wymbs, N.F., Grafton, S.T., 2014. Learning-induced autonomy of sensorimotor systems. arXiv 1403, pp. 6034.

Bassett, D.S., Yang, M., Wymbs, N.F., Grafton, S.T., 2015. Learning-induced autonomy of sensorimotor systems. Nat. Neurosci. 18, 744–751.

Betzel, R.F., Byrge, L., He, Y., Goñi, J., Zuo, X.-N., Sporns, O., 2014. Changes in structural and functional connectivity among resting-state networks across the human lifespan. NeuroImage 102, 345–357.

Blondel, V.D., Guillaume, J.L., Lambiotte, R., Lefebvre, E., 2008. Fast unfolding of community hierarchies in large networks. J. Stat. Mech., P10008.

Bullmore, E., Sporns, O., 2012. The economy of brain network organization. Nat. Rev. Neurosci. 13, 336–349.

Cabeza, R., Anderson, N.D., Locantore, J.K., McIntosh, A.R., 2002. Aging gracefully: compensatory brain activity in high-performing older adults. NeuroImage 17, 1394–1402.

Calhoun, V.D., Miller, R., Pearlson, G., Adalı, T., 2014. The chronnectome: time-varying connectivity networks as the next frontier in fMRI data discovery. Neuron 84, 262–274.

Cepeda, N.J., Kramer, A.F., Gonzalez de Sather, J., 2001. Changes in executive control across the life span: examination of task-switching performance. Dev. Psychol. 37, 715.

Chan, M.Y., Park, D.C., Savalia, N.K., Petersen, S.E., Wig, G.S., 2014. Decreased segregation of brain systems across the healthy adult lifespan. Proc. Natl. Acad. Sci. 111, E4997–E5006.

Cohen, J.R., Gallen, C.L., Jacobs, E.G., Lee, T.G., D'Esposito, M., 2014. Quantifying the reconfiguration of intrinsic networks during working memory. PLoS One 9, e106636.

Cole, M.W., Reynolds, J.R., Power, J.D., Repovs, G., Anticevic, A., Braver, T.S., 2013. Multi-task connectivity reveals flexible hubs for adaptive task control. Nat. Neurosci. 16, 1348–1355.

Cole, M.W., Bassett, D.S., Power, J.D., Braver, T.S., Petersen, S.E., 2014. Intrinsic and task-evoked network architectures of the human brain. Neuron 83, 238–251.

Contreras, J.A., Goñi, J., Risacher, S.L., Sporns, O., Saykin, A.J., 2015. The structural and functional connectome and prediction of risk for cognitive impairment in older adults. Curr. Behav. Neurosci. Rep. 2, 234–245.

Davison, E.N., Schlesinger, K.J., Bassett, D.S., Lynall, M.-E., Miller, M.B., Grafton, S.T., Carlson, J.M., 2015. Brain network adaptability across task states. PLoS Comput. Biol. 11, e1004029.

Dennis, E.L., Thompson, P.M., 2014. Functional brain connectivity using fMRI in aging and Alzheimer's disease. Neuropsychol. Rev. 24, 49–62.

Di, X., Biswal, B.B., 2015. Dynamic brain functional connectivity modulated by resting-state networks. Brain Struct. Funct. 220, 37–46.

Dubois, J., 2016. Brain age: a state-of-mind? On the stability of functional connectivity across behavioral states. J. Neurosci. 36, 2325–2328.

Ferreira, L.K., Regina, A.C.B., Kovacevic, N., Martin, M.d.G.M., Santos, P.P., Godoi Carneiro de C., Kerr, D.S., Amaro, E., McIntosh, A.R., Busatto, G.F., 2015. Aging effects on whole-brain functional connectivity in adults free of cognitive and psychiatric disorders, Cereb. Cortex. bhv190.

Folstein, M.F., Folstein, S.E., McHugh, P.R., 1975. Mini-Mental State: a practical method for grading the cognitive state of patients for the clinician. J. Psychiatr. Res. 12, 189–198.

Fortunato, S., Barthelemy, M., 2007. Resolution limit in community detection. Proc. Natl. Acad. Sci. 104, 36–41.

Geerligs, L., Renken, R.J., Saliasi, E., Maurits, N.M., Lorist, M.M., 2015. A brain-wide study of age-related changes in functional connectivity. Cereb. Cortex 25, 1987–1999.

Gomez-Ramirez, J., Li, Y., Wu, Q., Wu, J., 2015. A quantitative study of network robustness in resting-state fMRI in young and elder adults. Front. Aging Neurosci. 7.

Gonzalez-Castillo, J., Handwerker, D.A., Robinson, M.E., Hoy, C.W., Buchanan, L.C., Saad, Z.S., Bandettini, P.A., 2014. The spatial structure of resting state connectivity stability on the scale of minutes. Front. Neurosci. 8, 138.

Grady, C.L., Craik, F.I., 2000. Changes in memory processing with age. Curr. Opin. Neurobiol. 10, 224–231.

Grady, C., Sarraf, S., Saverino, C., Campbell, K., 2016. Age differences in the functional interactions among the default, frontoparietal control, and dorsal attention

networks. Neurobiol. Aging 41, 159–172.
Grady, C.L., 2008. Cognitive neuroscience of aging. Ann. N.Y. Acad. Sci. 1124, 127–144.
Grinsted, A., Moore, J.C., Jevrejeva, S., 2004. Application of the cross wavelet transform and wavelet coherence to geophysical time series. Nonlinear Process. Geophys. 11, 561–566.
Gu, S., Pasqualetti, F., Cieslak, M., Grafton, S.T., Bassett, D.S., 2014. Controllability of Brain Networks. arXiv preprint arXiv:1406.5197
Hagmann, P., Cammoun, L., Gigandet, X., Meuli, R., Honey, C.J., Wedeen, V.J., Sporns, O., 2008. Mapping the structural core of human cerebral cortex. PLoS Biol. 6, e159.
Hansen, E.C., Battaglia, D., Spiegler, A., Deco, G., Jirsa, V.K., 2015. Functional connectivity dynamics: modeling the switching behavior of the resting state. NeuroImage 105, 525–535.
Jacoby, L.L., Bishara, A.J., Hessels, S., Toth, J.P., 2005. Aging, subjective experience, and cognitive control: dramatic false remembering by older adults. J. Exp. Psychol.: General 134, 131.
Jenkinson, M., Beckmann, C.F., Behrens, T.E., Woolrich, M.W., Smith, S.M., 2012. FSL. NeuroImage 62, 782–790.
Meunier, D., Achard, S., Morcom, A., Bullmore, E., 2008. Age-related changes in modular organization of human brain functional networks. NeuroImage 44, 715–723.
Mucha, P.J., Richardson, T., Macon, K., Porter, M.A., Onnela, J.-P., 2010. Community structure in time-dependent, multiscale, and multiplex networks. Science 328, 876–878.
Ng, K.K., Lo, J.C., Lim, J.K., Chee, M.W., Zhou, J., 2016. Reduced functional segregation between the default mode network and the executive control network in healthy older adults: a longitudinal study. NeuroImage 133, 321–330.
Onoda, K., Ishihara, M., Yamaguchi, S., 2012. Decreased functional connectivity by aging is associated with cognitive decline. J. Cogn. Neurosci. 24, 2186–2198.
Power, J.D., Cohen, A.L., Nelson, S.M., Wig, G.S., Barnes, K.A., Church, J.A., Vogel, A.C., Laumann, T.O., Miezin, F.M., Schlaggar, B.L., et al., 2011. Functional network organization of the human brain. Neuron 72, 665–678.
Power, J.D., Schlaggar, B.L., Lessov-Schlaggar, C.N., Petersen, S.E., 2013. Evidence for hubs in human functional brain networks. Neuron 79, 798–813.
Qin, J., Chen, S.-G., Hu, D., Zeng, L.-L., Fan, Y.-M., Chen, X.-P., Shen, H., 2015. Predicting individual brain maturity using dynamic functional connectivity. Front. Hum. Neurosci. 9.
Sadaghlani, S., D'Esposito, M., 2015. Functional characterization of the cingulo-opercular network in the maintenance of tonic alertness. Cereb. Cortex 25, 2763–2773.
Sala-Llonch, R., Junqué, C., Arenaza-Urquijo, E.M., Vidal-Piñeiro, D., Valls-Pedret, C., Palacios, E.M., Domènech, S., Salvà, A., Bargalló, N., Bartrés-Faz, D., 2014. Changes in whole-brain functional networks and memory performance in aging. Neurobiol. Aging 35, 2193–2202.
Sala-Llonch, R., Bartrés-Faz, D., Junqué, C., 2015. Reorganization of brain networks in aging: a review of functional connectivity studies. Front. Psychol. 6.
Siebenhühner, F., Weiss, S.A., Coppola, R., Weinberger, D.R., Bassett, D.S., 2013. Intra- and inter-frequency brain network structure in health and schizophrenia. PLoS One 8, e72351.
Song, J., Birn, R.M., Boly, M., Meier, T.B., Nair, V.A., Meyerand, M.E., Prabhakaran, V., 2014. Age-related reorganizational changes in modularity and functional connectivity of human brain networks. Brain Connectivity 4, 662–676.
Tomasi, D., Volkow, N.D., 2012. Aging and functional brain networks. Mol. Psychiatry 17, 549–558.
Traud, A.L., Kelsic, E.D., Mucha, P.J., Porter, M.A., 2011. Comparing community structure to characteristics in online collegiate social networks. SIAM Rev. 53, 526–543.
Treitz, F.H., Heyder, K., Daum, I., 2007. Differential course of executive control changes during normal aging. Aging Neuropsychol. Cogn. 14, 370–393.
Turner, B.O., Lopez, B., Santander, T., Miller, M.B., 2015. One dataset, many conclusions: BOLD variability's complicated relationships with age and motion artifacts. Brain Imaging Behav. 9, 115–127.
Vossel, S., Geng, J.J., Fink, G.R., 2014. Dorsal and ventral attention systems: distinct neural circuits but collaborative roles. Neuroscientist 20, 150–159.
Wang, L., Su, L., Shen, H., Hu, D., 2012. Decoding lifespan changes of the human brain using resting-state functional connectivity MRI. PLoS One 7, e44530.
West, R., Murphy, K.J., Armilio, M.L., Craik, F.I., Stuss, D.T., 2002. Lapses of intention and performance variability reveal age-related increases in fluctuations of executive control. Brain Cogn. 49, 402–419.
Zalesky, A., Fornito, A., Cocchi, L., Gollo, L.L., Breakspear, M., 2014. Time-resolved resting-state brain networks. Proc. Natl. Acad. Sci. 111, 10341–10346.
Zhang, H.-Y., Chen, W.-X., Jiao, Y., Xu, Y., Zhang, X.-R., Wu, J.-T., 2014. Selective vulnerability related to aging in large-scale resting brain networks. PLoS One 9, e108807.